# NET RECHARGE DEPENDENCY ON LAND COVER TYPE

YULIANA GINTING
February, 2013

SUPERVISORS:
Dr. Ir. M.W. Lubczynski
Dr. Z. Vekerdy

ADVISOR:
Msc. Enrico Balugani (Ph.D Candidate)

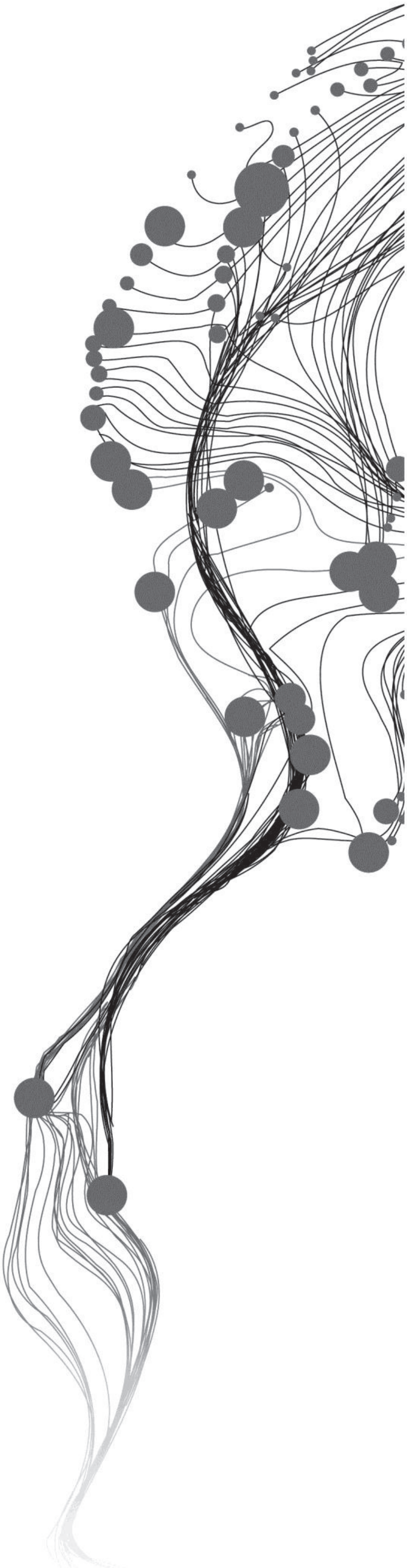

# NET RECHARGE DEPENDENCY ON LAND COVER TYPE

YULIANA GINTING
Enschede, The Netherlands, February 2013

Thesis submitted to the Faculty of Geo-Information Science and Earth Observation of the University of Twente in partial fulfilment of the requirements for the degree of Master of Science in Geo-information Science and Earth Observation.
Specialization: Water resources and Environmental Management

SUPERVISORS:
Dr. Ir. M.W. Lubczynski
Dr. Z. Vekerdy

THESIS ASSESSMENT BOARD:
Prof. Dr. Z. (Bob) Su (Chairman)
Prof. Dr. Li Jia (External Examiner, Alterra Univeristeit Wageningen)

DISCLAIMER
This document describes work undertaken as part of a programme of study at the Faculty of Geo-Information Science and Earth Observation of the University of Twente. All views and opinions expressed therein remain the sole responsibility of the author, and do not necessarily represent those of the Faculty.

# ABSTRACT

Groundwater is an important renewable resource. The largest freshwater in the earth, about 95%, is stored as groundwater. According to Dripps and Bradbury (2007) recharge is the entry of water into saturated zone. Therefore responsible for replenishment of groundwater  But in dry climate such as in semi-arid condition, groundwater evapotranspiration ($ET_g$) is high and is reducing the recharge ($R_g$). The difference between $R_g$ and $ET_g$ called net recharge ($R_n$) determines replenishment of groundwater resources and therefore also the sustainability of groundwater resources (Lubczynski, 2006). The aim of this research is to assess the dependency of net recharge on land cover type in the Sardón catchment in Spain.

A small patch (419,3 m x 239,3 m) within the Sardón catchment has been selected as NRZ (NRZ). The total area of the NRZ was 10039 $m^2$ which consisted of 93889 $m^2$ of bare soil, 4110 $m^2$ of *Quercus ilex* and 2340 $m^2$ of *Quercus pyrenaica* . The NRZ has uniform soil type and water table depth required to focus the research on dependency of net recharge on the land cover type. The net recharge of different land cover types within the NRZ is modeled using HYDRUS 1D.  HYDRUS 1D numerically solves the Richards equation and simulates water flow in the unsaturated zone. Simulations were performed in two different periods. The first period was used for calibration and it simulated 142 days, starting from 08/02/2009 until 29/06/2009. The second period was used for validation, simulating 162 days starting from 28/12/2009 until 07/06/2010. In order to compare the soil water fluxes in year 2009 (calibration period) and year 2010 (validation period), from both time series we chose the same periods starting at 15th February until 7th June to perform the model simulation

In both years the net recharge was negative. In 2009 the values of the net recharge were -203.29 mm for bare soil,   -0.03 mm for *Quercus ilex* and -0.02 mm for *Quercus pyrenaica*. In 2010 the values of net recharge were -165.00 mm for bare soil, -58.9 mm for *Quercus ilex* and -53 mm for *Quercus pyrenaica*. The negative value of the net recharge for both selected years means the $ET_g$ in this area was much higher than the recharge mainly at bare soil land cover type. This observation is understandable because the NRZ is located in the discharge zone of the Sardón catchment. The differences between net recharge responses at the three different land cover zones imply that the land cover type has a great impact on net recharge and furthermore on groundwater resources.

# ACKNOWLEDGEMENTS

The foremost I thank my supervisors, Dr. Ir. M.W. Lubczynski for the guidance and most of all, your patience, and Dr. Z. Vekerdy for sharing the new knowledge. Thank them for their supports until I finished my thesis. I would like to thank to my advisor, Enrico Balugani for being supportive and give valuable remarks to the work. I also want to thank to the research group in the Sardón catchment for all the suggestion and assistance during this period. I extend my gratitude to Dr. Boudewijn de Smeth for his guidance during the laboratory stage.

I would like to thank to all lectures and staffs especially WREM department, and also all ITC staffs for all the supports during my study. Thanks also to all my classmates WREM (2011-2013) for sharing me the sadness, happiness, and experiences.

Thanks to Nuffic Neso for giving me the chance to study in the Netherlands. To my Indonesian friends, Nahdya Maulina, Mulya Utami, Muhammad Kurniawan, Rizki Agung Nugroho, Edward Mengko, Nendi Rohaendi, Ahmat Sofatul Maki, Abdul Malik and Ari Sulistyo, thank you being a home when I'm far from home. It is unforgetable memory with all of you here.

I dedicate this thesis for my parents and my family in Indonesia. Without your supports, I would not be able to through the hard moments. Last but not least I want to thank Jesus, for without You I can't go this far.

My sincere thanks for all whom I mentioned here.

# TABLE OF CONTENTS

# LIST OF FIGURES

# LIST OF TABLES

# 1. INTRODUCTION

## 1.1. Background

Groundwater is one of the most important renewable resources. The largest freshwater in the earth, about 95% is stored as groundwater. The fact that two billions of people depend on fresh groundwater (United Nations Environment Programme, 2003) makes groundwater essential for human life. Therefore, sustainability of groundwater is an important issue, but vulnerable to many factors.

According to Dripps and Bradbury (2007) recharge is the entry of water into saturated zone. Therefore, it is responsible for replenishment of groundwater. But in dry climate such as in semi-arid condition, groundwater evapotranspiration ($ET_g$) is high and it's reducing the recharge ($R_g$).

$$R_n = R_g - ET_g \tag{1}$$

The $R_g$ is the amount of water which infiltrates through the soil and reaches the aquifer The $ET_g$ is the groundwater loss due to the process of transpiration (groundwater transpiration, $T_g$) and direct evaporation from water table (groundwater evaporation, $ET_g$). The difference between $R_g$ and $ET_g$ is called net recharge ($R_n$) determines replenishment of groundwater resources and therefore also the sustainability of groundwater resources (Lubczynski, 2006).

## 1.2. Research problem

Sardón catchment is a semi-arid region located in Spain, selected as the study area for this research. The net recharge in Sardón catchment is highly spatially variable because of the heterogeneity of land cover and subsurface (Lubczynski & Gurwin, 2005). However till now, there has not been research quantifying dependency of $R_n$ on land cover type.

## 1.3. Research objectives

To quantify the net recharge on groundwater resources under different land cover types in semi-arid, Sardón catchment area.

**Specific objectives**

1. To classify various land cover types present in Sardón catchment.
2. To build and calibrate 1-D hydrological models for each land cover type present in Sardón catchment.
3. To upscale calibrated net recharge into the plot scale.

## 1.4. Research questions

**General research question**

How dependent is net recharge on land cover type?

**Specific research questions**

1. How does net recharge vary per each land cover type?
2. What is the spatial and temporal variability of the net recharge at the selected plot?

## 1.5. Assumption

- There is no groundwater abstraction in the study area.
- The rate of the net recharge is uniform within each selected land cover zone.
- The non-vertical water fluxes in the soil in the area can be neglected.
- In the net recharge zone (NZR) water table depth is always the same at any instant in the whole area and change in time consequently.

# 2. STUDY AREA

## 2.1. Previous works in the Sardón study area

Many researches worked in Sardón catchment area for over last decade. Most of the studies were focused on transpiration, groundwater recharge modeling, groundwater resources evaluation and groundwater modeling e.g (Agbakpe, 2010; Cisneros Vaca, 2011; Llorono, 2000; Lubczynski & Gurwin, 2005; Ratnayake, 2000).

Deme (2011) assessed spatial and temporal subsurface fluxes in La Mata catchment.(~5 km$^2$), which is one of the sub-catchments of the Sardón catchment. La Mata catchment was divided into 12 zones based on hydraulic head, soil thickness, soil texture and surface elevation. HYDRUS 1D calculated the fluxes at the bottom of the soil for each zone and MODFLOW receives the fluxes as the recharge. MODFLOW calculated a new water table depth for the time step which assigns as the new pressure head at the bottom of the soil profile in the HYDRUS 1D for the next MODFLOW time step. The total subsurface fluxes are 0.302 mmd$^{-1}$ in September 2009 and 0.311 mmd$^{-1}$ in September 2010.

In the same area of La Mata catchment, (Effendi, 2012) compared two different evapotranspiration approaches, remote sensing (RS) using SEBS and Simple Energy balance and hydrological model approach using HYDRUS 1D to simulate evapotranspiration in La Mata catchment that focusing on dry season. Also Eddy covariance (EC) which is one of direct methods to calculate evapotranspiration was used to validate these two approaches. The result showed that generally actual evapotranspiration (AET) value from RS approach was higher than the value achieve by HYDRUS 1D and HYDRUS 1D give better agreement with EC method than RS approach. At time of the satellite overpass in 2009 the average AET values were 0,632, 0.667 and 0.392 mmd-1 for the SEBS, the Simple Energy Balance and HYDRUS 1D and in 2010 the average AET values were 0.156, 0.995 and 0,218 mmd-1. The information of subsurface fluxes is important to obtain reliable information of net recharge

## 2.2. Location

Sardón Catchment is located in Salamanca Province, central western Spain (Fig.1). The area is approximately 80 km$^2$ and lies between latitudes 41° 01'-41° 08N and 6° 07'- 6° 13' W. The altitude is about 740 m.a.s.l at the Sardón river outlet and 840 m.a.s.l at the southern boundary. The geomorphology of the study area consist of two different parts, a gentler undulating western and a steeper undulating eastern, the two are divided by the Sardón fault (Lubczynski & Gurwin, 2005)

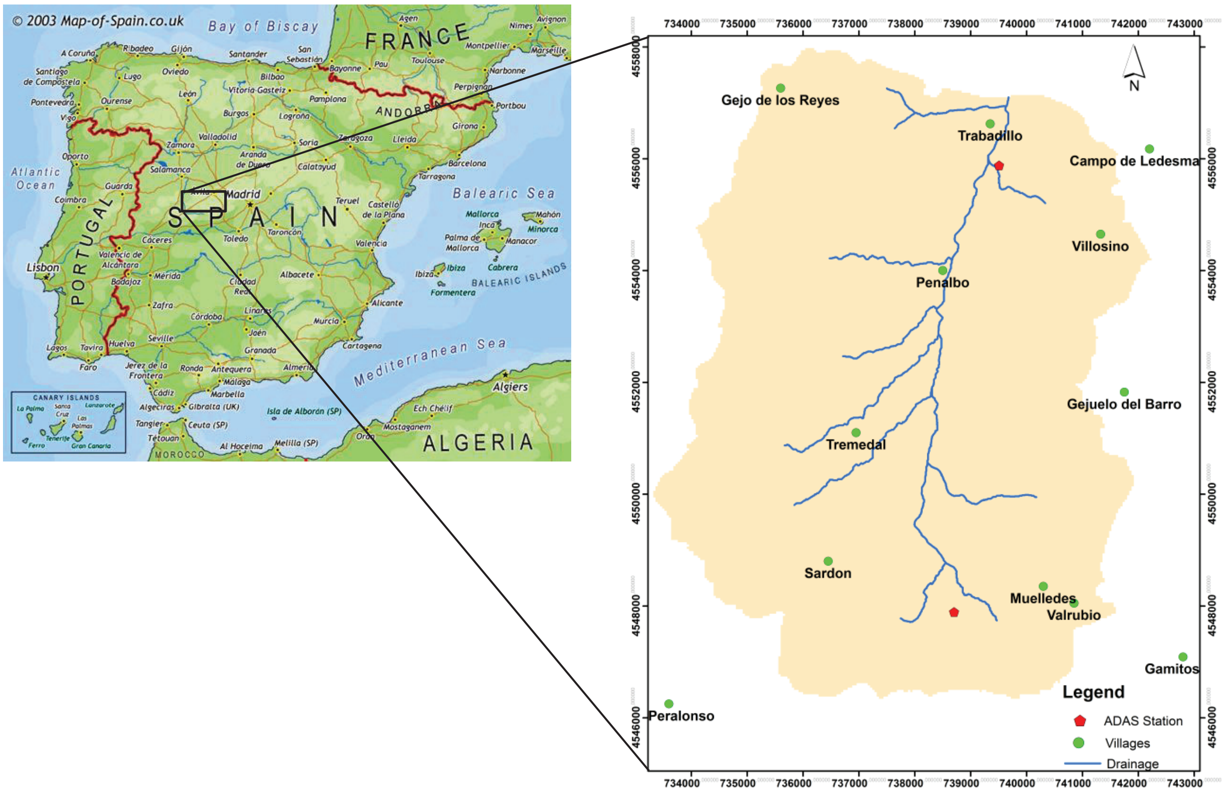

Figure 2-1. Location of the Sardón catchment study area.

## 2.3. Climate Condition

Sardón catchment is located in semi-arid climate. January and February are the coldest months with the average temperature are 5° C (Fig. 2). July and August are the warmest and the driest periods. The average temperature in this period is 22° C, rainfall is less than 20 mm/month and the average potential evapotranspiration is 5 mm/day. November and December are usually the wettest month with the average rainfall 100 mm/month and potential evaporation in December which on average 0.5 mm/d (Lubczynski & Gurwin, 2005)

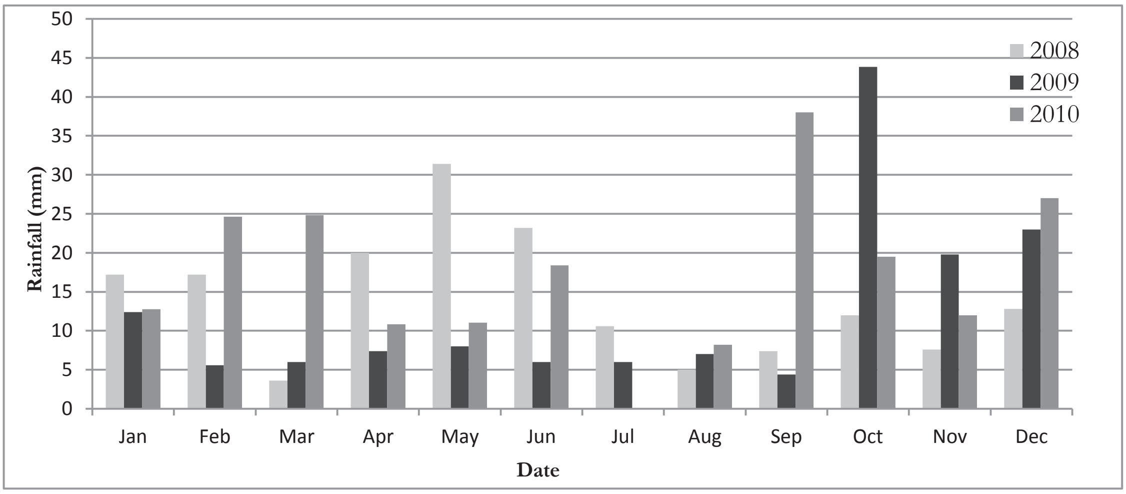

Figure 2-2. Rainfall in study area for 2008-2010.

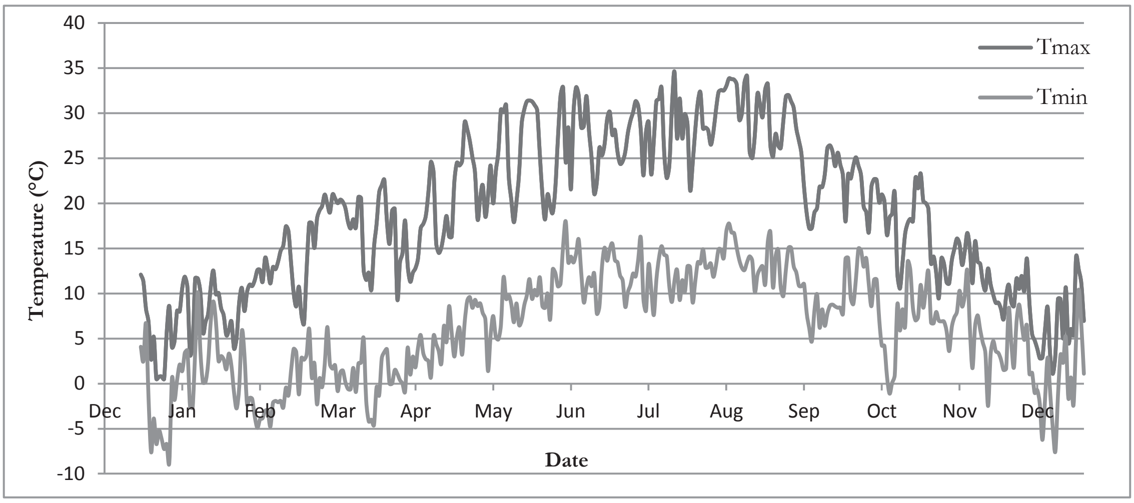

Figure 2-3. Temperature pattern in study area for 2009.

## 2.4. Land Cover and Land use

The soil product of granite weathering is generally unsuitable for agriculture and therefore the area is mainly used for pasture. In Sardón catchment the land cover is characterized by natural woody-shrub vegetation. There are two trees species in the study area (Figure 2.4). First is *Quercus ilex (Q.i)*, which is in Sardón it grows up to 6 m in average. Second is *Quercus pyrenaica (Q.p)*, a deciduous tree that has similar heightwith the trunk of approximately 0.4 m in diameter (Mutasa, 2011). The *Quercus pyrenaica* have a dense root system up to 60 cm. The trees are sparsely distributed in the study area and the area under the sparsely distributed trees is covered, *Citius scoparius* shrub and short grass (Shakya, 2001) which in the dry season is become bare soil. The tree canopies cover 7% of the study area with *Quercus ilex* covering 5% whilst *Quercus pyrenaica* cover 2%.

## 2.5. Hydrological Monitoring Network

Sardón catchment is monitored using ADAS station (Automated Data Acquisition Systems) located in Muelledes and Trabadillo (Fig.1). ADAS station is a monitoring system composed of multi sensors operated by data loggers. In this study ADAS station provided climate variables (rainfall, wind speed, solar radiation, relative humidity, temperature), stream discharges and groundwater table, in digital format.

## 2.6. Hydrogeology

The hydrogeology of Sardón catchment is influenced by weathering and fracturing processes. There are three layers that were identified in the study area; the top layer is unconsolidated layer, composed of weathered and alluvial deposit, and has thickness about 0-5 m. The second layer is fractured granite layer with intercalations of granodiorities, schist, gneisses. The third layer is massive granite layer with some gneiss inclusion that forms aquiclude. The groundwater table is influenced by the Sardón fault-river drainage line. The pattern of groundwater table is concentric and natural condition because in the groundwater use in the study area is negligible. The depth of groundwater table varies from 0-3 m b.g.s in the river valleys and 2-6 m b.g.s at the watershed boundaries. (Lubczynski & Gurwin, 2005).

Figure 2-4. Land cover in study area (a) bare soil, (b) *Quercus ilex* and (c) *Quercus pyrenaica* trees.

# 3. MATERIAL AND METHOD

## 3.1. Literature Review

Recharge is one of the most important components in the asssesment of groundwater resources. There are already numerous researches about techniques to quantify recharge (Anuraga et al., 2006; Dripps & Bradbury, 2007; Finch, 1998). These techniques also have been described widely, for example Scanlon et al. (2002) divided recharge estimation techniques based on three hydrological zone; surface water, unsaturated zone, and saturated zone and within each zone techniques were generally classified into physical, tracer, or numerical modeling approaches. Among the recharge methods, modeling of water fluxes in unsaturated zone is one of the common approaches to estimate recharge.

There are many approaches to simulate water movement in the unsaturated zone, for instance soil-water storage-routing approaches, quasi-analytical approaches and numerical solutions to the Richards equation. Examples of codes that use the Richards equation include BREATH, HYDRUS-1D, HYDRUS-2D, SWIM, VS2DT and UNSATH (Scanlon et al., 2002).

In quantifying recharge with numerical modeling in unsaturated zone, it is important to consider the effect of vegetation. Vegetation has impact in redistribution of precipitation by vegetation canopy; provide preferential flow, and the roots extract water from the unsaturated zone, etc (Le Maitre et al., 1999). In modeling of root water uptake, there are two major approaches that are generally used; microscopic (or mesoscopic) approach and macroscopic approach (Feddes & Raats, 2004). Microscopic approach considers a single root uptake while macroscopic approach assumes root as a zone, neglecting the root geometry and preferential flow around the root. Because macroscopic approach is simpler than the microscopic approach, the macroscopic approach is more commonly used in unsaturated zone modeling than the microscopic approach

## 3.2. General Methodology

The general methodology for this study is illustrated in Figure 3-1. The spatial and temporal (net recharge zone) NRZ is modeled using HYDRUS-1D with input of soil hydraulic properties, meteorological data and root water uptake parameter.

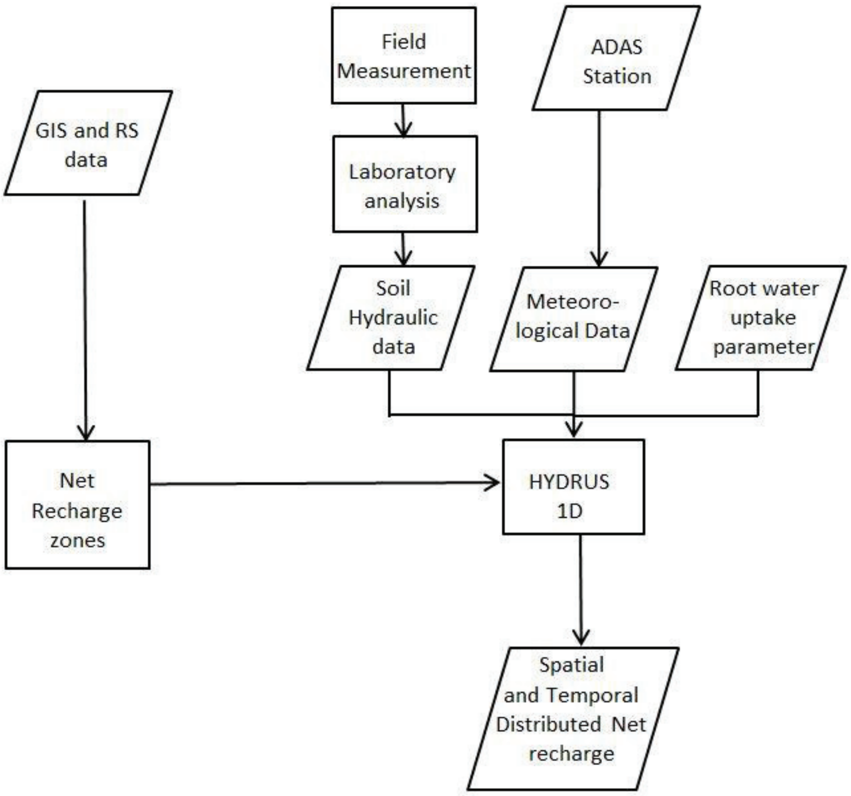

Figure 3-1. Flowchart of general methodology for this study.

### 3.3. Net Recharge Zonation Based on Remote Sensing

There are two high resolution, multispectral (4 bands) images available for the study area, Quick Bird acquired on 9th August 2011 (dry season) and WorldView II acquired on 1$^{st}$ December 2011 (wet season). From these high resolution images, tree species classification has been done by Leonardo Reyes (Reyes-Acosta & Lubczynski, 2013). Three land cover units were identified through GIS data processing. These are 1) bare soil, 2) area under *Quercus ilex* canopy and 3) area of *Quercus pyrenaica* canopy. The land cover classification of this study is presented in Figure 3.2. Each identified land cover unit represents specific Rn zone that is further modeled using the HYDRUS 1D model. In figure 3-2 the yellow box presents selected recharge zonation plot with 3 land cover types, each modeled using HYDRUS 1D. The HYDRUS 1D solution is dependent on water table depth therefore plot selection was made in a way to guarantee uniform water table depth within the plot in order to focus the research on dependency of net recharge on the land cover type only.

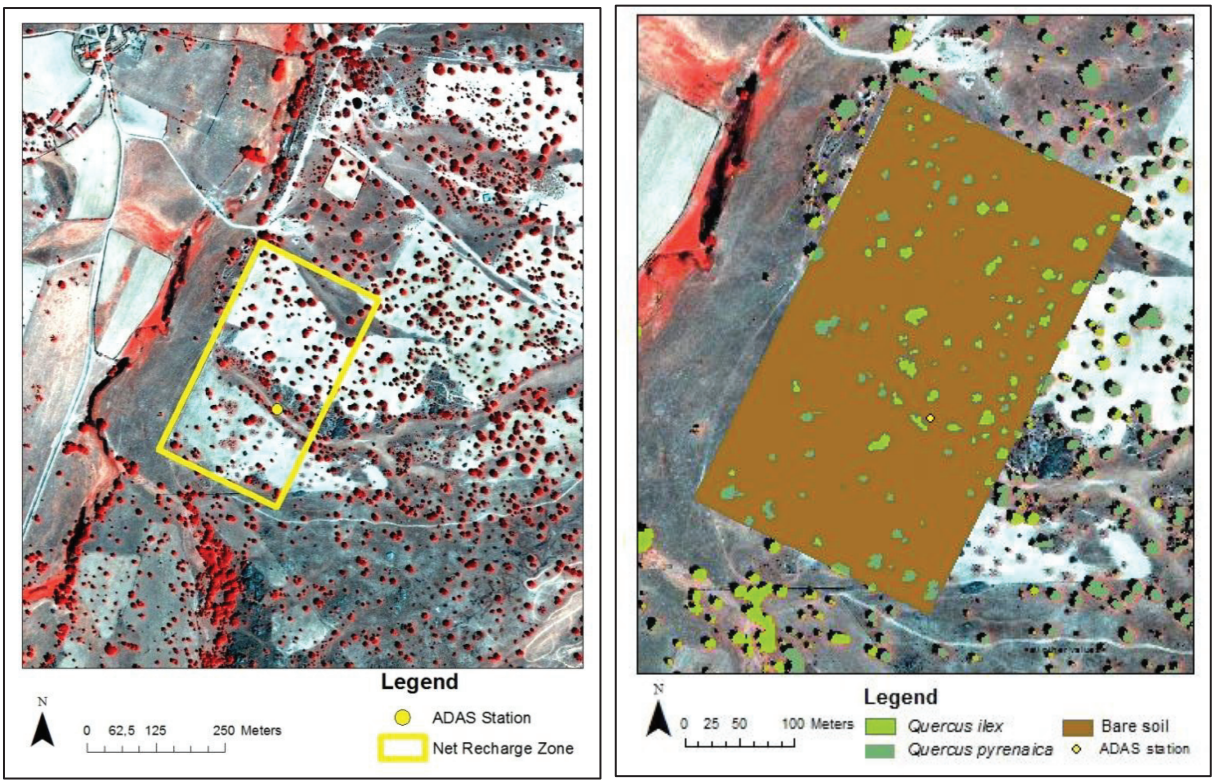

Figure 3-2. Net recharge zonation (419,3 m x 239,3 m)from Quick Bird image (left) and land cover map (right).

### 3.3.1. HYDRUS 1D Parameterization

- **Soil Hydraulic properties**

To model the water flow in unsaturated zone, we have to understand the hydraulic properties of the soil in that particular soil. We collected information of the soil hydraulic properties by taking soil samples and analyzing them in the laboratory. The soil sampling, both vertically in the profile and spatially in the area, is useful to understand the heterogeneity of the soil in the study area.

#### *Field Measurement*

In the available database at ITC, there is sufficient information on hydraulic properties of the weathered rock (regolith) therefore the fieldwork sampling was focused on the alluvium part of the study area. Sampling was done using hand augering and excavation. 14 soil sample bags and 15 soil sample rings were collected. Further, soil samples were analyzed in laboratory to obtain properties.

#### *Laboratory Analysis*

Particle size test was done for the soil sample bag to get the percentage of sand, silt and clay. This information later was used as input to ROSETTA, software which implements pedotransfer functions, to produce the hydraulic properties required by the soil hydraulic parameters model used (in this case, van Genuchten (1980)).

Permeameter test were performed using soil sample ring to get their saturated conductivity. The tests conducted with the permeameter were either constant head method, in case of a sample with medium to high saturated hydraulic conductivity, or falling head method in case of samples with low saturated hydraulic conductivity.

### Statistical analysis

To assess the heterogeneity of the soil in the study area, we performed some basic statistical analysis. The soils were divided into two group based on from where they were taken, i.e. either from regolith or alluvium area. In each group we calculated the mean of percentage of gravel, sand, clay, and silt to check the null hypothesis “the means and standard deviation of the two groups are the same” i.e. “the two soils have the same hydraulic parameters”. The result of soil analysis is presented in *Chapter 4, Result and discussion.*

- **Meteorological parameters**

Meteorological parameters are needed to calculate potential evaporation (PET) using Penman-Monteith (P-M) method. The meteorological parameters needed are radiation parameter, wind speed, temperature and the height at which they were collected.

- **Tree specific land cover parameters**

The area under the vegetation needs additional information related to surface fraction/(LAI) leaf area index such as:

#### ***Surface fraction/ LAI (leaf area index*).**

To calculate PET in area under vegetation we need the information of surface fraction/LAI. LAI value is obtained from the literature. LAI of *Quercus ilex* around 4,6 $m^2m^{-2}$-5,3 $m^2m^{-2}$ (Sala et al., 1994) and LAI of *Quercus Pyrenaica* is around 0,12 $m^2m^{-2}$-1,86 $m^2m^{-2}$ (Riano et al., 2004).

#### ***Interception***

Not all the water from the precipitation reaches the soil surface and infiltrate through the soil. Some of the water from precipitation is caught by surface storage (vegetation canopy) and evaporates before it reaches the soil. Interception differs depending on the vegetation type; because different vegetation types have different leaves shape, thickness, distribution, arrangement and etc. In this study area, interception has been measured from the 23 October 2011 until 9 august 2012 by Tanvir Hassan (Ph.D. candidate). In HYDRUS 1D interception is modeled using the following equation:

$$I = a \; x \; LAI \left[ 1 - \frac{1}{1+\frac{SFC\,.\,P}{a\,.\,LAI}} \right] \tag{2}$$

Where *I* is interception, *a* is interception constant, *LAI* is leaf area index, *SFC* is surface fraction and *P* is precipitation. Because in this study the value of interception constant was unknown, the interception measurements are used to fit pattern of interception calculated by HYDRUS 1D for *Quercus ilex* and the *Quercus pyrenaica* patterns. Trial and error method is used to achieve the fitting: HYDRUS 1D *I* parameter is varied until the interception pattern modeled resembles the measured one.

- **Root Parameter**

The potential root water uptake distribution is time independent; however, the root water uptake rate itself may be time dependent To calculate the water uptake from the vegetation we have to specify the spatial distribution of the potential root water uptake, that depends on the tree physiology and roots distribution (Šimůnek et al., 2012). We specify the spatial root distribution by defining the spatial region of the root zone in the soil profile and the relative intensity of the potential root water uptake distribution. Besides root distribution, also the following parameters of water stress response had to be specified: the pressure head at which the root water uptake is reduced by 50% and the experimental constants ($p_0$). These parameters were specified by trial and error method because of limited information from the literature and because there was no available measurement

### 3.3.2. Temporal Variable

- **Meteorological Data**

From the ADAS station we obtained meteorological variables which are needed to calculate potential evapotranspiration and more in general, the upper boundary condition. Meteorological data needed are net radiation, maximum and minimum temperature, air humidity and wind speed and precipitation.

- **Groundwater Table**

Groundwater table data were recorded by a pressure transducer installed in a piezometer close to the ADAS station and was representative for the selected plot (Figure 3-2). Groundwater table data were used as lower boundary condition, with the lower boundary condition set as given variable pressure head.

## 3.4. HYDRUS 1D Simulation

To estimate the net recharge we used the model HYDRUS 1D. HYDRUS 1D program numerically solves Richards Equation (Eq. 3) and simulates water flow in the unsaturated zone.
The Richard's equation is:

$$\frac{\partial\theta}{\partial t} = \frac{\partial}{\partial z}\left[K\left(\frac{\partial h}{\partial z} + cos(\alpha)\right)\right] - S \tag{3}$$

Where $h$ is the pressure head [L], $\theta$ is the volumetric water content $[L^3L^{-3}]$, t is time [T], $x$ is the spatial coordinate [L] (positive upward), $S$ is the sink/source term $[L^3L^{-3}T^{-1}]$, $a$ is the angle between the flow direction and the vertical axis, and $K$ is the unsaturated hydraulic conductivity.

### 3.4.1. Soil Hydraulic Model

The relationship of pressure head and soil moisture content is described by retention curve. The retention curve is affected by the structure of the soil matric. Sandy soil and clay soil have different behavior. To make the retention curve for a particular soil type HYDRUS 1D permits to select within five different soil hydraulic properties models, which are Van Genuchten-Mualem, modified Van Genuchten, Brooks-Corey and Kosugi. In this study we used Van Genuchen-Mualem (van Genuchten, 1980) because for prediction of soil hydraulic conductivities this model is the most widely used in literature (Simunek et al., 2012). This model is describe below

$$\theta(h) = \theta_r + \frac{\theta_s - \theta}{[\,(1+\alpha h)^{\,n}\,]^{1-1/n}} \tag{4}$$

$\theta_r$ is the residual water contents
$\theta_s$ is the saturated water contents,
$a$ is the inverse of the air-entry value (or bubbling pressure) or the pressure head where air starts to enter the largest pore in the soil and
$n$ is a pore-size distribution index.

For the prediction of the hydraulic conductivity, Van Genuchten used the statistical pore-size distribution model (Mualem, 1976).

$$K(h) = K_S \, S_e{}^{l}[1-(1-S_e{}^{\frac{1}{1-1/n}}-)^{1-1/n}]^2 \qquad (5)$$

$K_s$ is the saturated hydraulic conductivity and *l* is a pore-connectivity. In many soils, the pore connectivity parameter was estimated (Mualem, 1976) to be about 0.5. Pore size distribution makes the soil doesn't mimic the permeability of a bundle of straight capillary tubes. But in the reality, there are many factor that make soil much more complex, such as twisted and crooked pores, dead-ending or connecting to other pores (Vervoort & Cattle, 2003). The parameters *a*, *n* and *l* in HYDRUS 1D are considered to be empirical coefficients affecting the shape of hydraulic function.

### 3.4.2. Root Water Uptake Model

In equation (3) the term *S* can be determined as volume of water removed from the soil at a particular depth due to root water uptake. Feddes define *S* as:

$$S(h) \;= \alpha\,(h)S_p \qquad (6)$$

Where *Sp* is the potential water uptake rate and *a (h)* is a prescribed dimensionless function of the soil water pressure which describe the response of water uptake by plant under stress. According to Van Genuchten the value *a (h)* follow the *S* shaped function. (Figure 3-5).

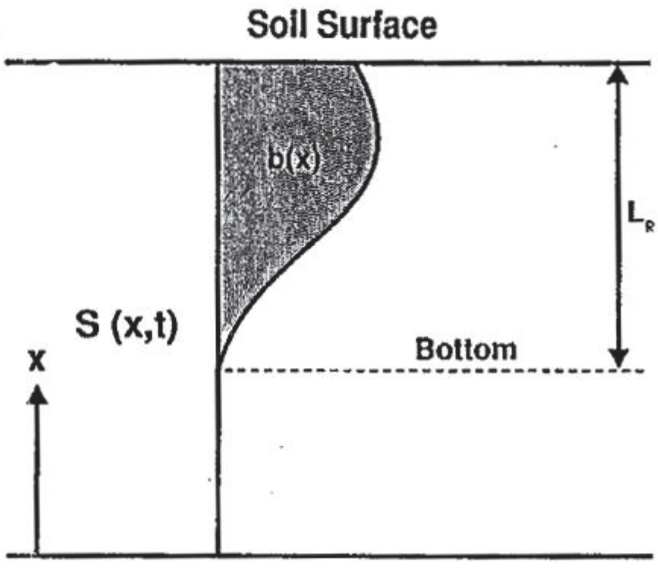

Figure 3-3. Schematic of the plant water response function based on Van Genuchten (1987) water uptake model (Šimůnek et al., 2012).

$$\alpha(h) = \frac{1}{1+(\frac{h}{h_{50}})^p} \qquad (7)$$

The parameter $h_{50}$ showed in the Figure 3.5 is the pressure head at which the water extraction rate is reduced by 50% during conditions of negligible osmotic stress.

When the potential water uptake rate is equally distributed over the root zone, $S_p$ becomes

$$S_p = \frac{1}{L_r} T_p \tag{8}$$

where $T_p$ is the potential transpiration rate [LT$^{-1}$] and $L_r$ is the depth of the root zone [L]. If the potential water uptake is not equally distribute over the root zone, $1/L_r$ may be generalized using a non-uniform distribution of the potential water uptake rate over an arbitrary shape of root zone:

$$S_p \ = \ b(x)Tp \tag{9}$$

$$b(x) = \frac{b'(x)\, dx}{\int_{L_r} b'(x) dx} \tag{10}$$

$$\int_{L_r} b(x) dx = 1 \tag{11}$$

where *b(x)* is the normalized water uptake distribution [L-$^{1}$] (Figure 3-5)

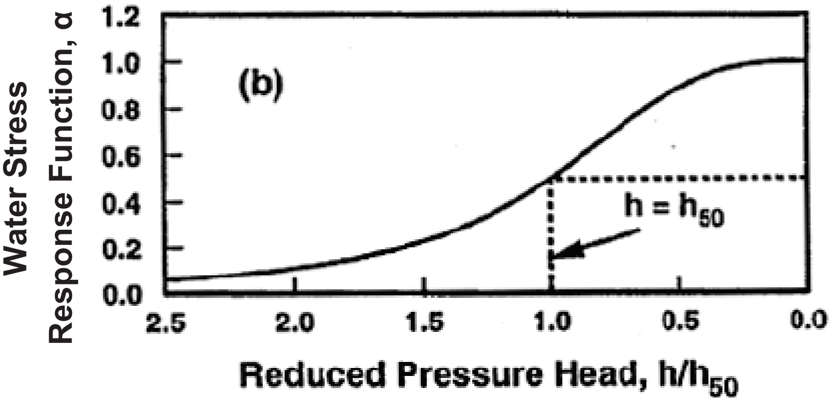

Figure 3-4. Potential water uptake distribution function, b(x), in the soil root zone (Šimůnek et al., 2012).

From equation (8) and equation ( 9) we can get

$$\int_{L_r} S_p \, dx = T_p \tag{12}$$

by substituting equation (8) to equation (3) we can obtain the actual water uptake distribution

$$S(h, x) = \alpha(h, x) \ b(x) T_p \tag{13}$$

The actual transpiration rate ($T_a$) is obtained by integrating the actual water uptake distribution (Šimůnek et al., 2012)

$$T_a = \int_{L_r} S(h, x) \ dx = Tp \int_{L_r} \alpha(h, x) \ b(x) dx \tag{14}$$

### 3.4.3. Penman-Monteith

Potential evaporation (ET0) is calculated using the Penman-Monteith method. $ET_0$ is determined using a equation that combines radiation and aerodynamic terms as follows:

$$ET_0 = ET_{rad} + ET_{aero} = \frac{1}{\lambda}\left[\frac{\Delta(R_n - G)}{\Delta+\gamma(1+r_c/r_a)} + \frac{\frac{\rho\, cp(e_a - e_d)}{r_a}}{\Delta+\gamma(1+r_c/r_a)}\right] \quad (15)$$

$$\Delta = \frac{4098\, ea}{(T+237.3)^2} \quad (16)$$

where all terms explained in table. 3-1

Table 3-1. Penman-Monteith parameter

| Notation | Description | Unit |
|---|---|---|
| ET$_0$ | Evapotranspiration rate | mm d$^{-1}$ |
| Et$_{rad}$ | Radiation term | mm d$^{-1}$ |
| Et$_{aero}$ | Aerodynamic term | mm d$^{-1}$ |
| $\lambda$ | Latent heat of vaporization | MJ kg$^{-1}$ |
| R$_n$ | Net radiation at surface | MJ m$^{-2}$d$^{-1}$ |
| G | Soil heat flux | MJ m$^{-2}$d$^{-1}$ |
| $\varrho$ | Atmospheric density | kg m-3 |
| c$_p$ | Specific heat of moist air | i.e., 1.013 kJ kg$^{-1}$ $^o$C$^{-1}$ |
| (e$_a$-e$_d$) | Vapor pressure deficit | kPa |
| e$_a$ | Saturation vapor pressure at temperature T | kPa |
| e$_d$ | Actual vapor pressure | kPa |
| r$_c$ | Crop canopy resistance | s m$^{-1}$ |
| r$_a$ | Aerodynamic resistance | s m$^{-1}$ |
| $\Delta$ | Slope of the vapor pressure curve | kPa $^o$C$^{-1}$ |
| $\gamma$ | Pressure curve | kPa |

### 3.4.4. Calibration control data –soil matric potential

Soil matric potential is measured in each land cover at five different depths using Watermark sensors installed in each profile at 25, 50, 75, 100 and 125 cm depth below the soil surface. Below (Figure 3-6-Figure 3-8) is the matric potential measurement in each land cover, the dashed black line represents the calibrationand validation periods.

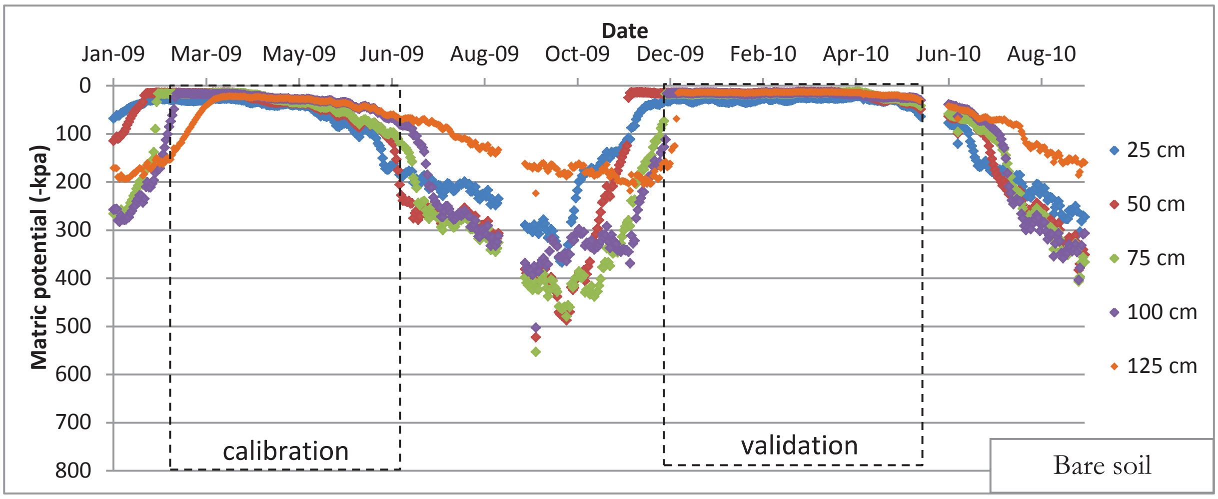

Figure 3-5. Soil matric potential measured in bare soil.

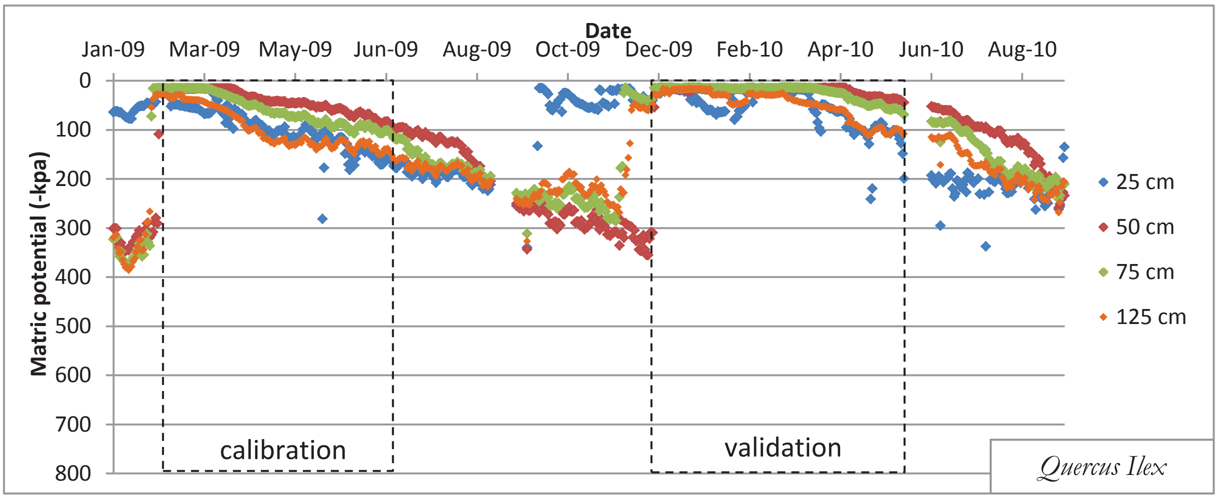

Figure 3-6. Soil matric potential measured in soil under *Quercus ilex*.

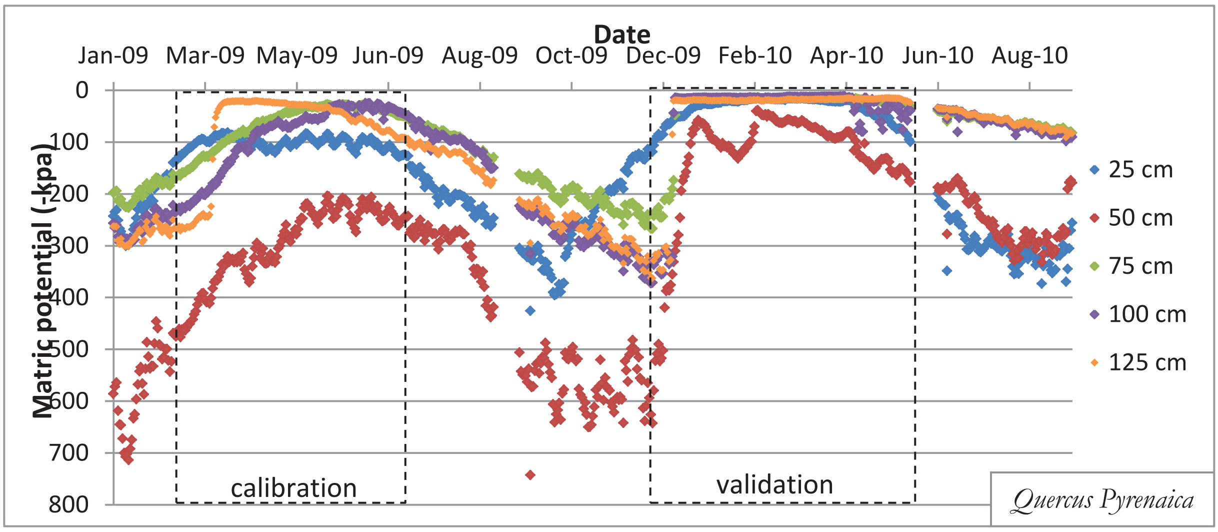

Figure 3-6. Soil matric potential measured in soil under *Quercus pyrenaica*

### 3.5. Model Calibration and Validation

Simulation was performed in two different periods. The first period is used for calibration and it simulates 142 days, starting from 08/02/2009 until 29/06/2009. The second period is used for validation, simulating 162 days starting from 28/12/2009 until 07/06/2010 and they are the best periods to detect any net recharge, due to the wet conditions (after the winter period) and the high precipitation rates. We also selected the 2 different years due to their difference in cumulative precipitation, 2009 being a relatively dry year and 2010 a relatively wet year. These periods were chosen based on the completeness of meteorological data as variable boundary conditions and also to depict maximum land cover change. The depth of soil profile was 321 cm, and it was based on the maximum depth of the piezometer, so also its groundwater table measurements that were used as the HYDRUS 1D lower boundary condition.

The soil profile is discretized into 321 nodes with atmospheric boundary conditions with surface layer as the upper boundary condition and variable pressure head as the lower boundary condition. The measurement of soil matric potential in the beginning of each simulation was used as initial condition.
Soil matric potential measurement was used for calibrating soil hydraulic properties and tree specific land cover parameters. The objective of the model calibration was to achieve a good agreement between the matric potential output of the model and the measured data. Trial and error was one of method to make model calibrated. Another approach was to use parameter estimation. In HYDRUS 1D, parameter estimation was performed using the Levenberg-Marquardt nonlinear minimization method (a weighted least-squares approach based on Marquardt's maximum neighborhood method).

An important measure of the goodness of fit is the $r^2$ value for regression of the observed, ŷi, versus fitted, yi(b), values:

$$r^2 = \frac{[\Sigma wi\,\hat{y}i\,yi - \frac{\Sigma\hat{y}i\,\Sigma yi}{\Sigma\,wi}]^2}{[\,\Sigma wi\,\hat{y}i^2 - \frac{(\Sigma\,\hat{y}i)^2}{\Sigma wi}][\,\Sigma yi^2 - \frac{(\Sigma\,yi)^2}{\Sigma wi}]} \tag{4}$$

The initial estimation of hydraulic properties is obtained from the soil measurement from the field. The parameter estimation is done by adding layer and tune the Van Genucthen parameters until simulation of matric potential has a good correlation ($r^2$ >0,7) with the observation measurement and is still close to the values actually observed in laboratory. During the parameter estimation process it is important to use different initial estimation value to prevent the local minimum objective function. In process calibration, trial and error is also used to find the best fit of tree specific parameter, since the data of these parameters are not available and difficult to find.

# 4. RESULT AND DISCUSSION

## 4.1. Soil Analysis

We collected 14 soil sample bags and 15 soil sample rings taken during the fieldwork campaign (Figure 4.1 and Figure 4.2). The soil texture analysis has been done for the 14 soil sample bags (figure 4-1 and table 4-1) and permeameter test has been done for the 15 soil sample rings (table 4-2). The aim of those analysis is to get the soil hydraulic properties for the input of the HYDRUS 1D model.

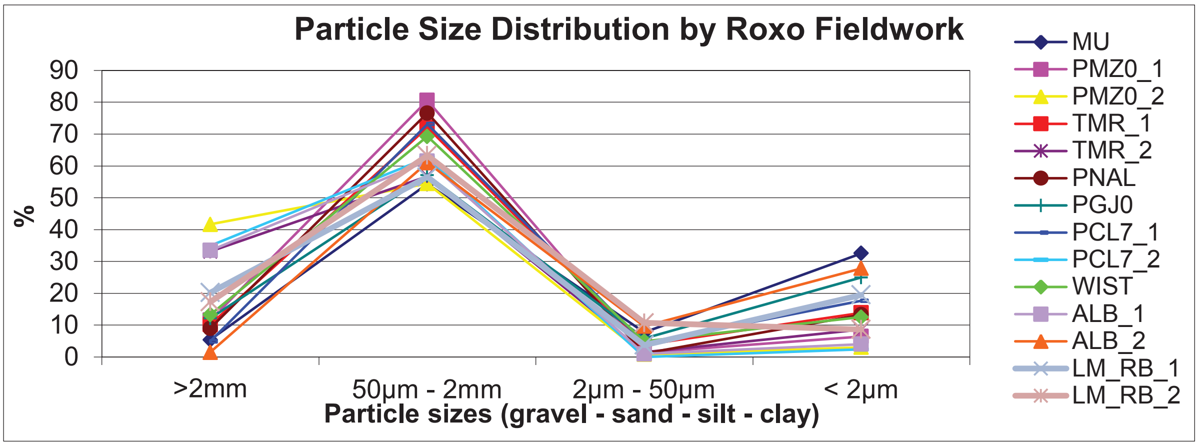

Figure 4-1. Particle size distribution of soil sample bags.

Table 4-1. Particle size analysis.

| No | Object ID | Coordinate UTM ED1950 X | Coordinate UTM ED1950 Y | GRAVEL (%) | SAND (%) | SILT (%) | CLAY (%) | Depth (cm) |
|---|---|---|---|---|---|---|---|---|
| 1 | MU | 739480 | 4547702 | 5.40 | 54.34 | 7.70 | 32.56 | 50 |
| 2 | PMZ0_1 | 739668 | 4557040 | 11.59 | 80.58 | 1.38 | 6.45 | 35 |
| 3 | PMZ0_2 | 739668 | 4557040 | 41.65 | 54.48 | 0.82 | 3.05 | 90 |
| 4 | TMR_1 | 737069 | 4551354 | 10.18 | 72.09 | 3.84 | 13.89 | 25-32 |
| 5 | TMR_2 | 737069 | 4551354 | 33.10 | 56.75 | 1.53 | 8.62 | 49-57 |
| 6 | PNAL | 738576 | 4553800 | 9.03 | 76.61 | 1.10 | 13.26 | 25-50 |
| 7 | PGJ0 | 736090 | 4557816 | 12.13 | 57.08 | 5.83 | 24.97 | 25-50 |
| 8 | PCL7_1 | 738395 | 4551359 | 4.91 | 73.15 | 4.28 | 17.66 | 25-50 |
| 9 | PCL7_2 | 738395 | 4551359 | 35.00 | 62.58 | 0.02 | 2.40 | 25-50 |
| 10 | WIST | 736348 | 4548953 | 13.27 | 69.29 | 4.92 | 12.52 | 13-18 |
| 11 | ALB_1 | 736100 | 4554211 | 33.45 | 61.53 | 0.98 | 4.04 | 30-35 |
| 12 | ALB_2 | 736100 | 4554211 | 1.47 | 61.03 | 9.68 | 27.82 | 40-45 |
| 13 | LM_RB_1 | 739669 | 4555972 | 20.20 | 56.54 | 3.75 | 19.51 | 40-45 |
| 14 | LM_RB_2 | 739669 | 4555972 | 17.32 | 63.29 | 10.71 | 8.68 | 110-115 |

Table 4-2. Saturated conductivity in 15 soil sample rings.

| No | Object ID | Coordinate UTM ED1950 | | Ksat (m/day) | Depth (cm) |
|---|---|---|---|---|---|
| | | X | Y | | |
| 1 | MU_5 | 739480 | 4547702 | 4,12 | 5 |
| 2 | MU_50 | 739480 | 4547702 | 0,58 | 50 |
| 3 | PNF_5 | 738434 | 4553756 | 1,06 | 5 |
| 4 | PNAL_5 | 738576 | 4553800 | 0,98 | 5 |
| 5 | BAR 5 | 741471 | 4551529 | 0,13 | 5 |
| 6 | Bar_5 field | 741418 | 4551537 | 0,77 | 5 |
| 7 | LM_R 5 | 739669 | 4555972 | 1,59 | 5 |
| 8 | LM_RB 5 | 739669 | 4555972 | 0,19 | 5 |
| 9 | PCL7_FL | 739023 | 4551936 | 145,70 | 5 |
| 10 | WIST_5 | 736348 | 4548953 | 0,01 | 5 |
| 11 | PMZ0_70 | 739668 | 4557040 | 0,5 | 70 |
| 12 | Sardon 5 | 736206 | 4548724 | 0,33 | 5 |
| 13 | AL_B2 5 | 736100 | 4554211 | 0,37 | 5 |
| 14 | PGJ0_5 | 736090 | 4557816 | 0,21 | 5 |
| 15 | TMR_5 | 737069 | 4551354 | 0,34 | 5 |

In the previous years soil analysis have also been performed in the Sardon study area (Cisneros Vaca, 2011; Deme, 2011; Effendi, 2012). These data were integrated with the dataset collected in the present study to make a basic for the statistical analysis to investigate the heterogeneity of soil in the study area. In the Figure 4-2, alluvium group is shown in blue color and regolith group in red color. The box plot shows that there is not much difference of the lower quartile, median, upper quartile, the smallest and the largest observation in two populations. From this analysis we can assume that the soil in the study area is homogeneous.

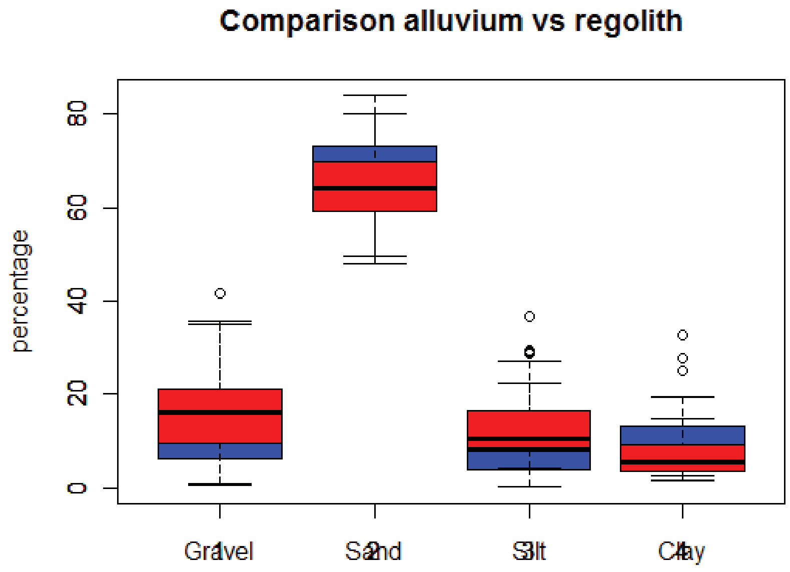

Figure 4-2. Percentage of gravel, sand, silt and clay in alluvium and regolith groups.

## 4.2. Model calibration and validation

The result of parameter estimation in tuning the Van Genucten parameter and soil profile for each of the three land cover models is presented in table 4-3.

Table 4-3. Van Genuchten parameter.

| Layer | Land cover | Van Genucthen parameter | | | | | | Depth of layer (cm) |
|---|---|---|---|---|---|---|---|---|
| | | θr | θs | α | n | Ks (cm/d) | l | |
| 1 | Bare soil | 0,020 | 0,41 | 0,010 | 1,46 | 75 | 0,5 | 0-98 |
| | *Quercus ilex* | 0,0200 | 0,41 | 0,020 | 1,33 | 52 | 0,5 | 0-39 |
| | *Quercus pyrenaica* | 0,0040 | 0,44 | 0,037 | 1,20 | 100 | 0,5 | 0-51 |
| 2 | Bare soil | 0,0390 | 0,33 | 0,014 | 2,97 | 160 | 0,5 | 98-119 |
| | *Quercus ilex* | 0,0390 | 0,39 | 0,020 | 2,70 | 110 | 0,5 | 39-80 |
| | *Quercus pyrenaica* | 0,0130 | 0,44 | 0,060 | 1,30 | 110 | 0,5 | 51-105 |
| 3 | Bare soil | 0,0840 | 0,33 | 0,001 | 1,50 | 250 | 0,5 | 119-158 |
| | *Quercus ilex* | 0,0840 | 0,33 | 0,010 | 1,50 | 230 | 0,5 | 80-125 |
| | *Quercus pyrenaica* | 0,0340 | 0,33 | 0,010 | 1,30 | 200 | 0,5 | 105-150 |
| 4 | Bare soil | 0,0037 | 0,4 | 0,030 | 4,30 | 55 | 0,5 | 158-321 |
| | *Quercus ilex* | 0,0037 | 0,4 | 0,04 | 4,3 | 59 | 0,5 | 125-321 |
| | *Quercus pyrenaica* | 0,0037 | 0,45 | 0,054 | 1,7 | 45 | 0,5 | 150-321 |

Using Van Genuchen parameters in table 4-3, the matching between observed and simulated soil matric in bare soil, soil covered by *Quercus ilex* and soil covered by *Quercus pyrenaica* are shown in figure 4-4, 4-5 and 4-6. The goodness of fit for both calibration and validation are summarized in table 4-4. For validation the goodness of fit is lower than in calibration, it might be because of two different characteristic of the year when for calibration we use data from 2009 which is in relative dry condition and for validation we use data from 2010 which is in wet condition.

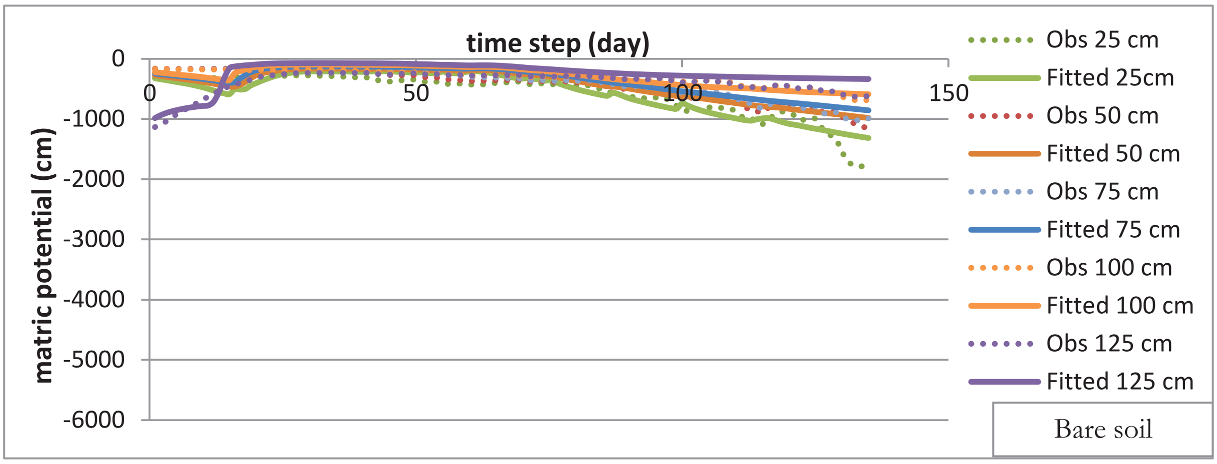

Figure 4-3. Observed vs simulated matric potential for bare soil.

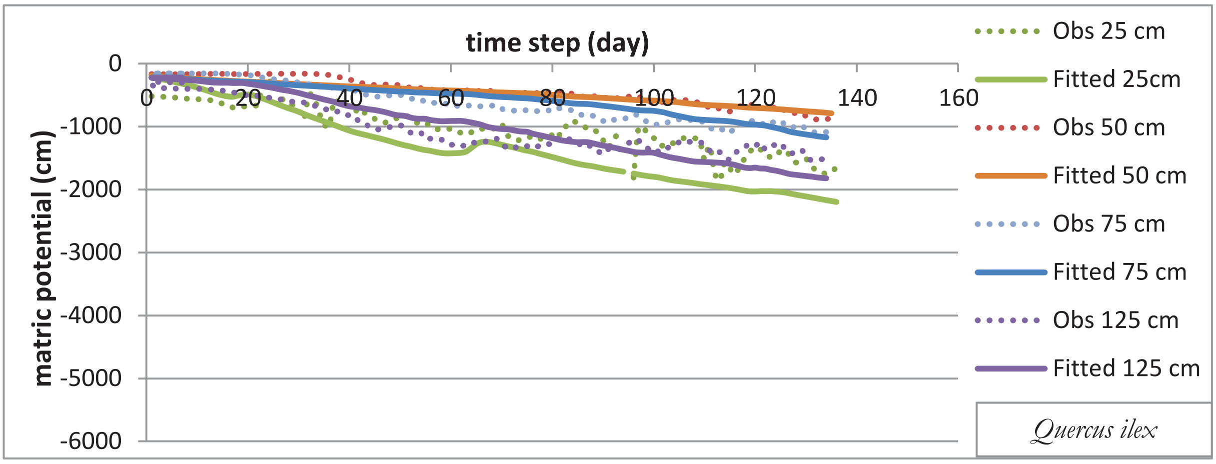

Figure 4-4. Observed vs simulated matric potential for *Quercus ilex*.

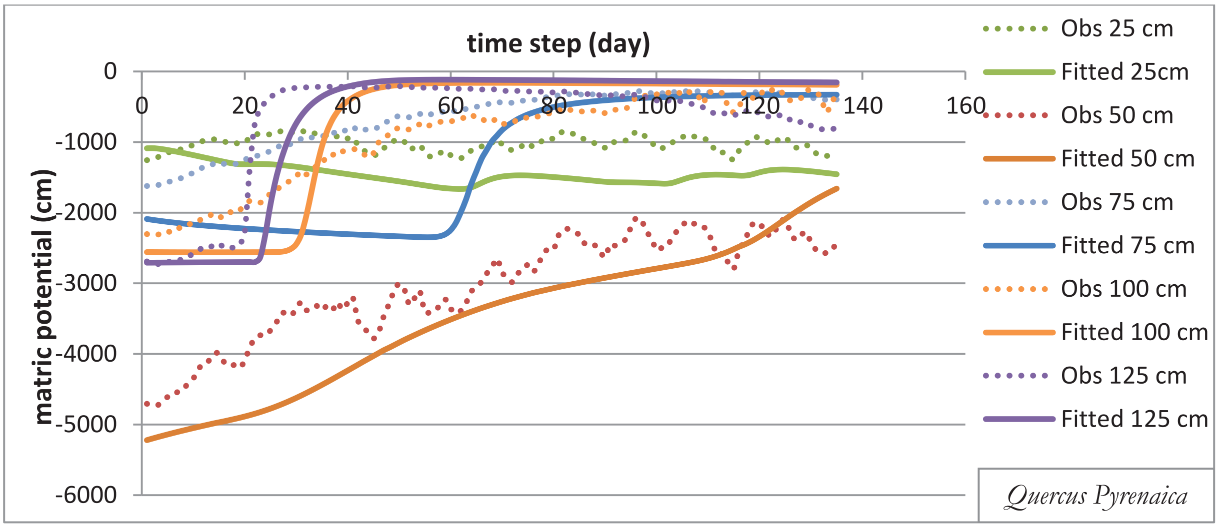

Figure 4-5. Observed vs simulated matric potential for *Quercus Pyrenaica*.

Table 4-4. The goodness of fit for calibration and validation.

| Land cover | $r^2$ | |
|---|---|---|
| | Calibration | Validation |
| Bare soil | 0,83 | 0,70 |
| *Quercus ilex* | 0,83 | 0,50 |
| *Quercus pyrenaica* | 0,86 | 0,64 |

## 4.3. Temporal Simulation

In order to compare the soil water fluxes in year 2009 (dry) and year 2010 (wet), we choose the same period starting at 15th February until 7th June to perform our simulation.

**Terms in this simulation**:

**Actual infiltration:** water that touches the first node [L].

**Actual evaporation**: evaporation that takes place in the first node [L].

**Actual surface flux (SF)**: evaporation-infiltration [L].

**Actual bottom flux (BF)**: inflow or outflow in the last node [L].

**Prescribed bottom pressure head (BPH):** bottom pressure head assigned for simulation [L].

**Actual bottom flux in constant upper boundary condition (CUBC)**: bottom flux when we simulate zero constant flux in upper boundary [L].

**In HYDRUS 1D (+) sign is for the upward flow and (-) sign is for the downward flow**.

### 4.3.1. Bare soil-2009

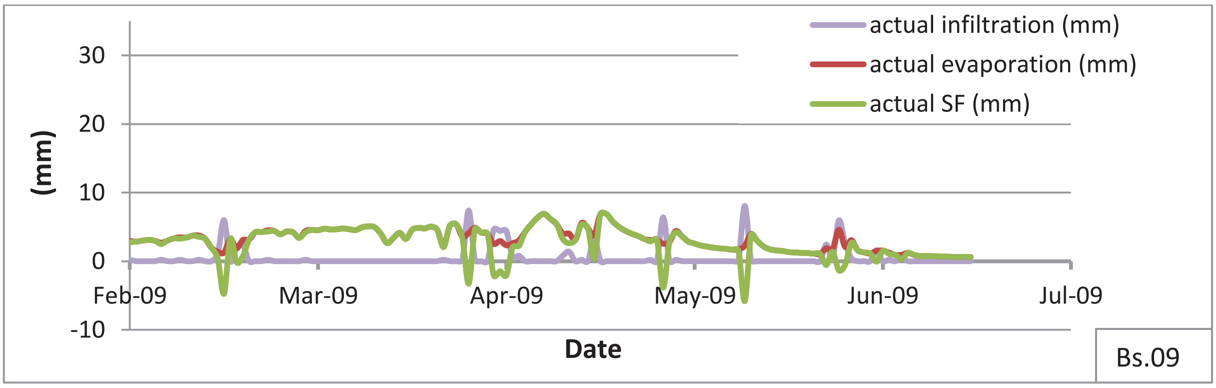

Figure 4-6. Comparison of actual infiltration, actual evaporation and actual SF for bare soil in 2009.

In figure 4-6 the purple line represents the infiltration, the red line is the evaporation and the green line is the actual SF. The evaporation process takes place throughout the simulation, becoming higher in February and March because of the water table rise which was close to the surface and getting lower due to the lowering of water table on April (figure 4-7). Since actual SF is infiltration minus evaporation in first node, therefore the negative value (downward flow) of the actual SF is the water that passes to the second node i.e. is the amount of water that possibly become recharge or net recharge.

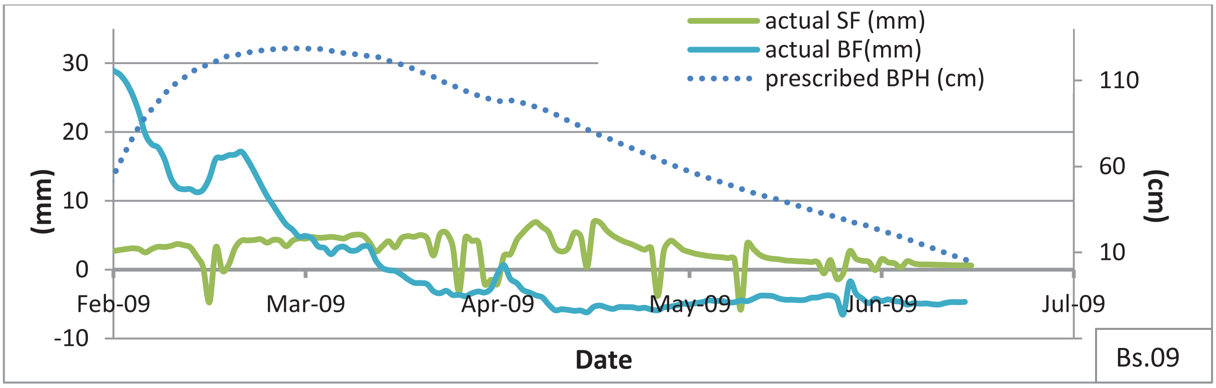

Figure 4-7. Comparison actual SF, actual BF and prescribed BHP for bare soil in 2009.

In figure 4-7 the green line shows the actual SF, the cyan line is the BF and the blue dot line is the prescribed BPH. We can see from the figure 4-7 that the BF seems not to react because of the SF but because of the variation of the BPH that was assigned as the lower boundary conditions.

To see the effect of bottom pressure head to the actual BF, we prescribed constant flux as the upper boundary condition (CUBC) and we assigned it zero. In figure 4-8, the cyan line is the BF in normal simulation and the orange line is the BF in CUBC simulation. Therefore, the difference between two of them is the effect of climatic condition in the surface. This difference is interpreted as the net recharge that shows as the blue line in the figure 4-8.

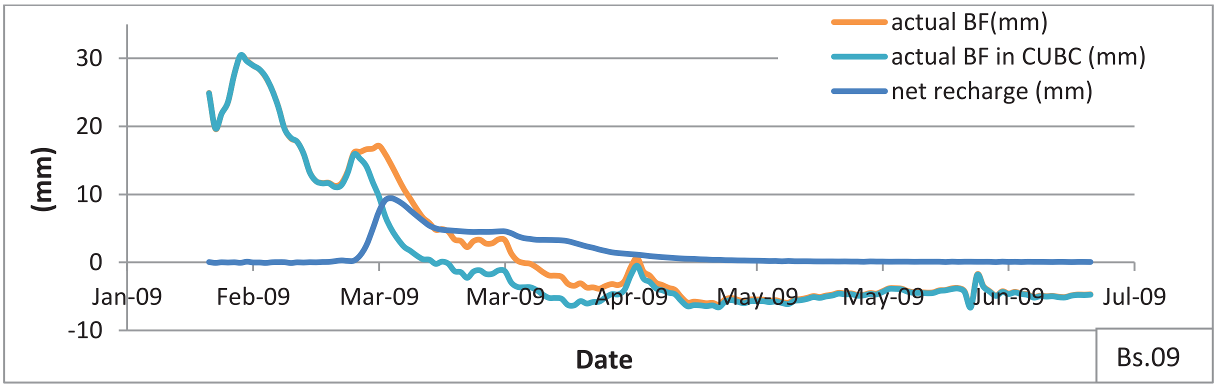

Figure 4-8. Comparison of actual BF, actual BF in CUBC and net recharge for bare soil in 2009.

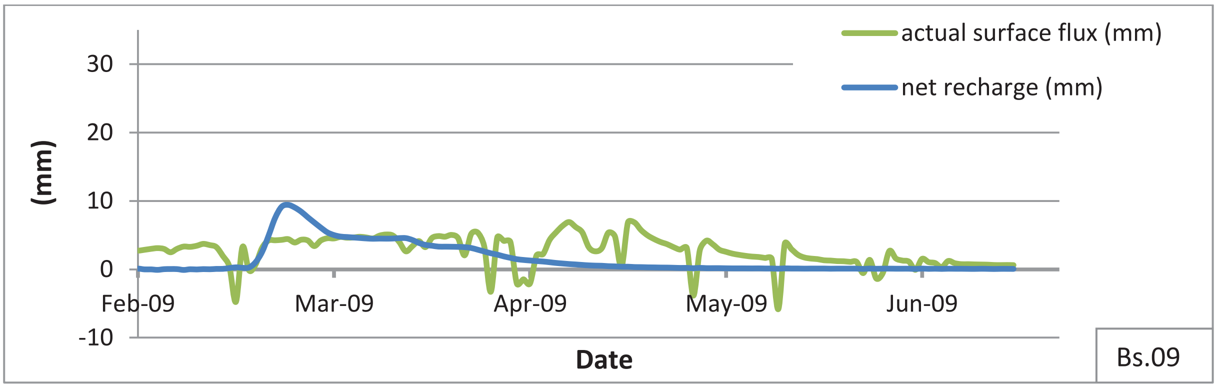

Figure 4-9. Comparison the actual surface flux and net recharge for bare soil in 2009.

In figure 4-9 the green line is the actual SF and the blue line is the net recharge. As we can see that water which passes the second node is already evaporated before reaches the bottom of the soil.

### 4.3.2. *Quercus ilex*-2009

In figure 4-10 the purple line represents the infiltration, the red line is the evaporation and the green line is the actual SF. Differently to what happens in the bare soil, in the soil covered by *Quercus ilex* the evaporation is lower. It may be because of the shading effect by the canopy. *Quercus ilex* is an evergreen tree that has leaves along the year; therefore its canopy can prevents solar radiation to reach the soil surface and to evaporate the water.

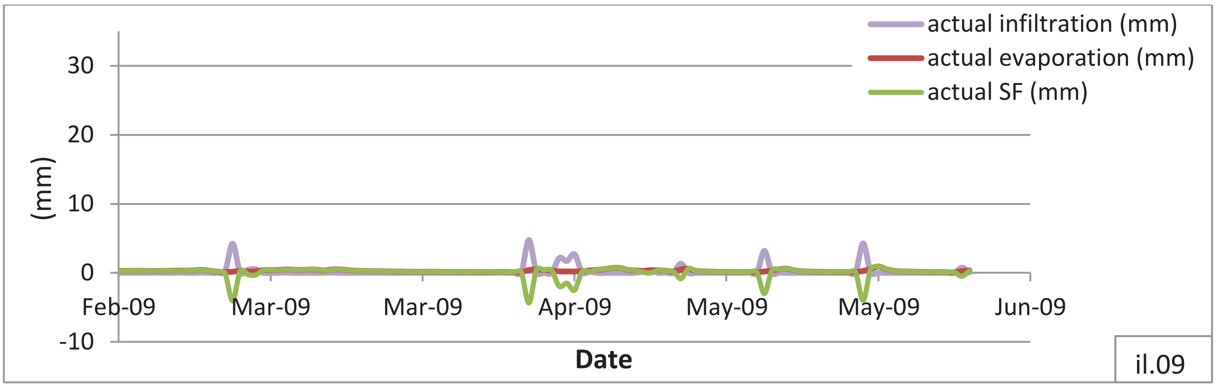

Figure 4-10. Comparison of actual infiltration, actual evaporation and actual SF for *Quercus ilex* in 2009.

In the figure 4-11 the green line is the actual SF, the black line is the root water uptake (RU) and the brown line is the SF added with the RU. Because the positive sign is referring to the evaporation which is loss of water, therefore the actual root water uptake, which is also sink or loss of water in soil, acts as an added value to the actual SF. The negative value of SF+RU can potentially be converted to recharge.

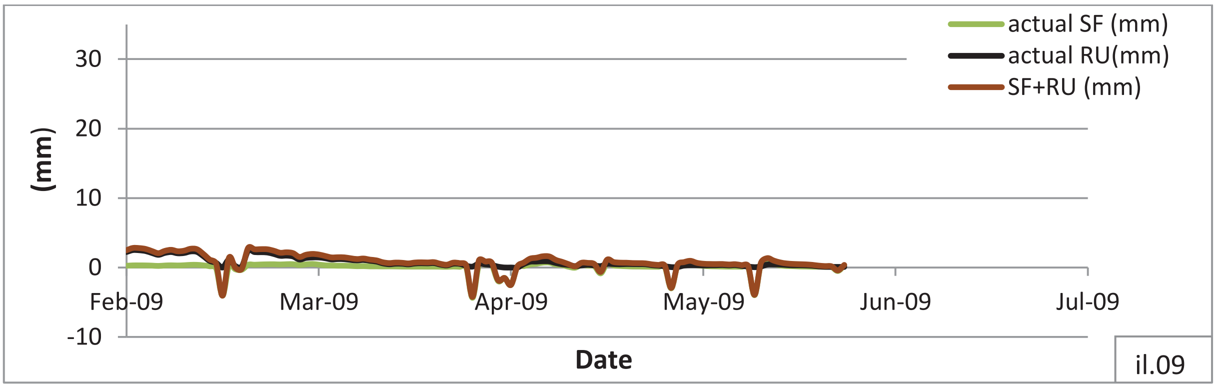

Figure 4-11. Comparison the actual SF, actual RU and the SF+RU for *Quercus ilex* in 2009.

In the figure 4-12 the green line shows the actual SF, the cyan line is the BF and the dot blue line is the prescribed BPH. The same situation as in bare soil can be observed: the BF seems not to react to the SF conditions but because of the variation of the BPH which assigned as lower boundary conditions. To see the effect of bottom pressure head to the BF, we did the same process as in bare soil: to simulate zero constant flux as the upper boundary condition (CUBC).

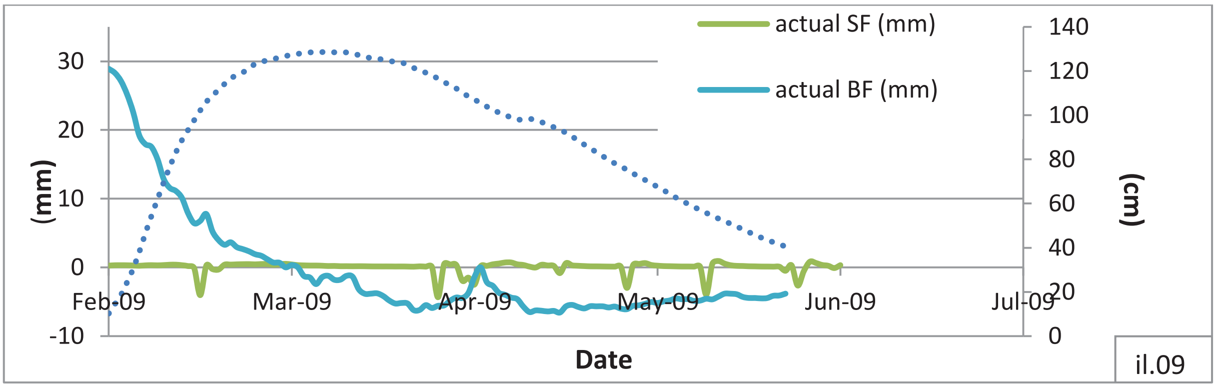

Figure 4-12. Comparison actual SF, actual BF and prescribed BHP for *Quercus ilex* in 2009.

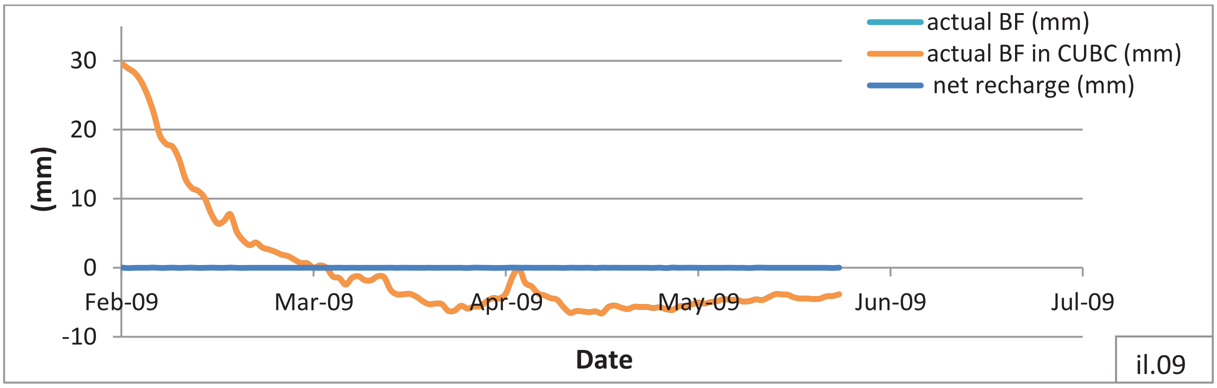

Figure 4-13. Comparison of actual BF, actual BF in CUBC and net recharge for *Quercus ilex* in 2009.

In figure 4-13, the actual BF shown in cyan color is perfectly overlapping with the BF in CUBC which shown in the orange line. It means that the BF is not affected by the evapotranspirative conditions such as surface flux or root water uptake. In this condition the net recharge is zero.

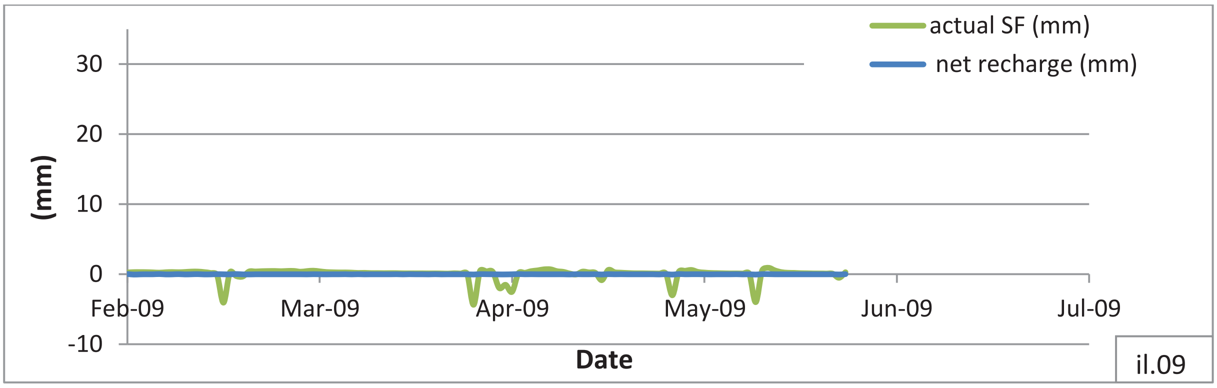

Figure 4-14. Comparison the actual surface flux and net recharge for *Quercus ilex* in 2009.

In figure 4-14 the green line is the SF and the blue line is the net recharge. As we can see water that passes to the second node (actual SF) is already evaporate or taking up by the tree before reaches the bottom of the soil profile.

### 4.3.3. *Quercus pyrenaica*-2009

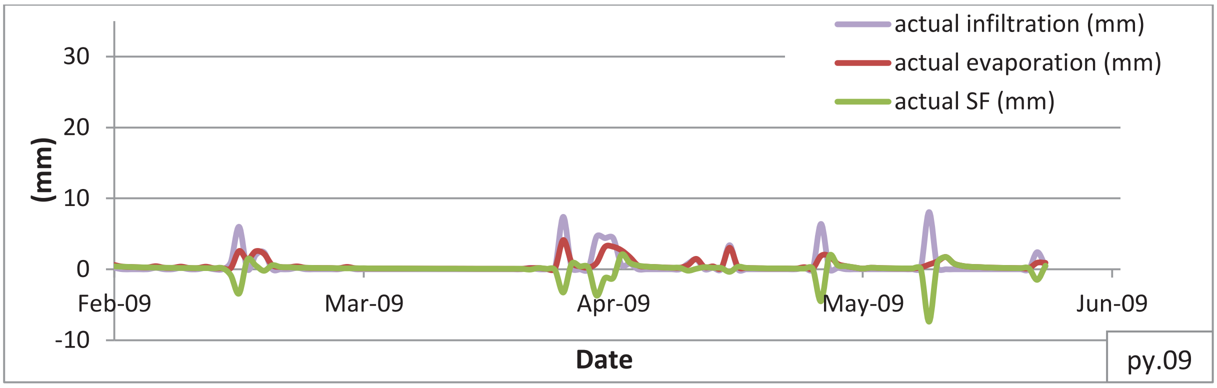

Figure 4-15. Comparison of actual infiltration, actual evaporation and actual SF for *Quercus pyrenaica* in 2009.

In figure 4-15 the purple line represents the infiltration, the red line is the evaporation and the green line is the actual surface flux. In this simulation the evaporation is also low, even though *Quercus pyrenaica* start to have canopy in 15th May. In the beginning, when the water table is deep, the unsaturated water starts to evaporate, because the initial condition in this simulation is relative drier than in bare soil, therefore the evaporation is also low. When the groundwater table rises there should be higher evaporation, but it is not may be because of the plant litter and residues that act as water repellency, according to Wang et al. (2000) a soil is less wettable if the soil is dry and contains organic matter. The inverse air entry value that can be used as one of indicator of soil water repellency is also higher than in bare soil.

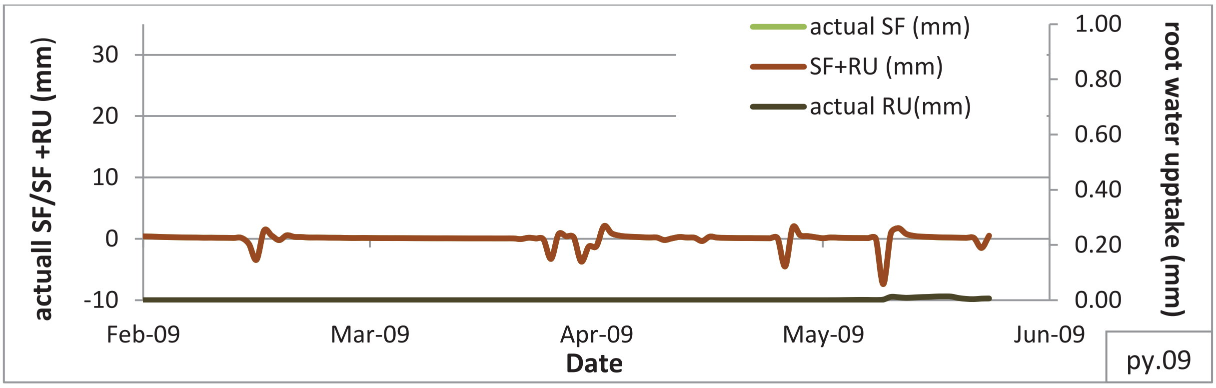

Figure 4-16. Comparison the actual SF, actual RU and the SF+RU for *Quercus pyrenaica* in 2009.

In the figure 4-16 the green line is referring to actual surface flux, the black line is the RU and the brown line is the SF+RU. From the figure we can see that the root water uptake is almost zero or a very small value. The root water uptake, of *Quercus pyrenaica* starts at 15th May; when the gets in leaves; finally the tree's roots started to uptake water, the groundwater table was already decreasing, hence the water was not taken up in the end.

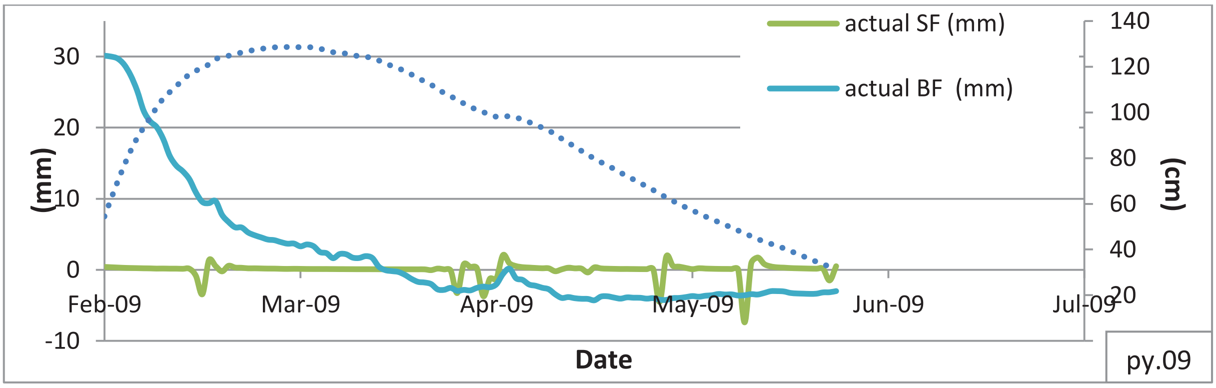

Figure 4-17. Comparison actual SF, actual BF and prescribed BHP for *Quercus pyrenaica* in 2009.

In Figure 4-17, we compare the actual SF, actual BF and prescribed BPH in Quercus pyrenaica to see wheater the actual BF is influenced by climatic condition in the surface (actual SF) or not. From the figure, it seems that the actual BF is more influenced by the prescribed BPH . To investigate more, we simulate the CUBC.

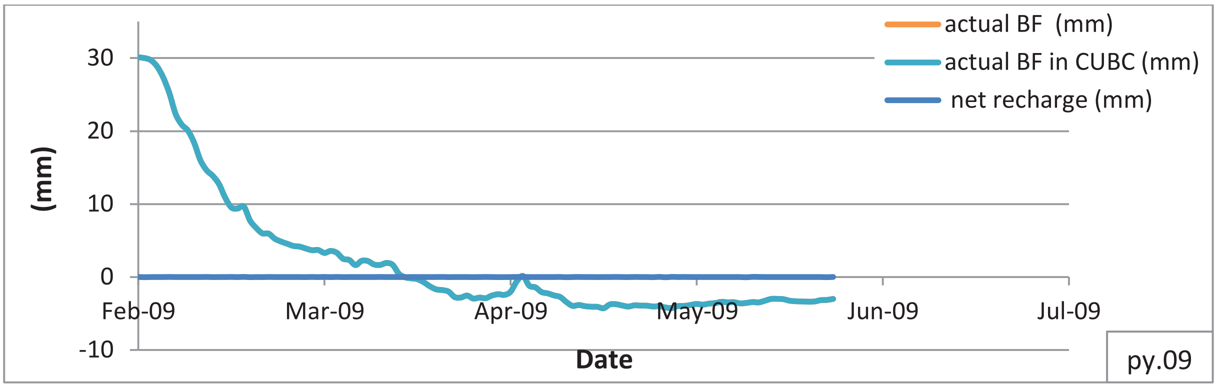

Figure 4-18. Comparison of actual BF, actual BF in CUBC and net recharge for *Quercus pyrenaica* in 2009.

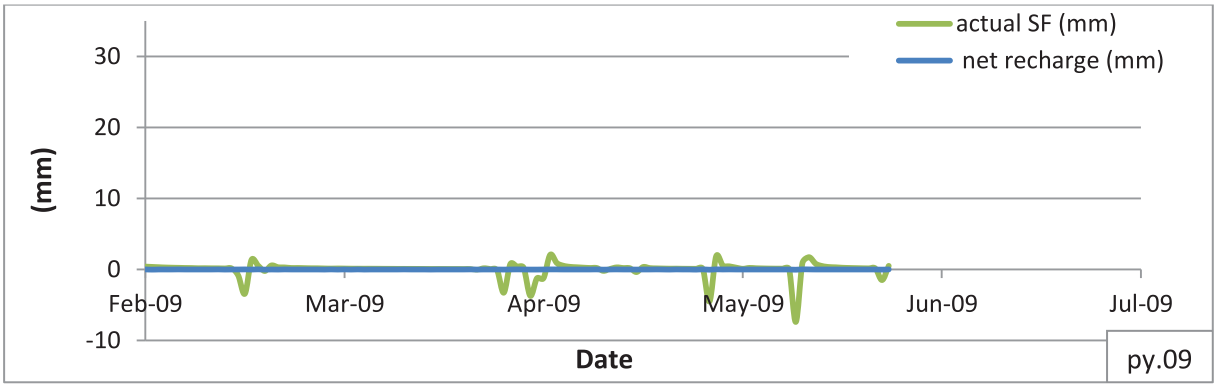

Figure 4-19. Comparison the actual SF and net recharge for *Quercus pyrenaica* in 2009.

In the figure 4-18 the actual BF shows in cyan color is also perfectly overlapping with the BF in CUBC which shows in the orange line. This is a similar situation with the model land covered by *Quercus ilex* . It means that the BF was not affected by the upper conditions (such as surface flux or root water uptake). In this condition the net recharge is zero. In figure 4-19 the green line is the SF and the blue line is the net recharge. As we can see the actual SF is not influence the net recharge.

### 4.3.4. Bare soil-2010

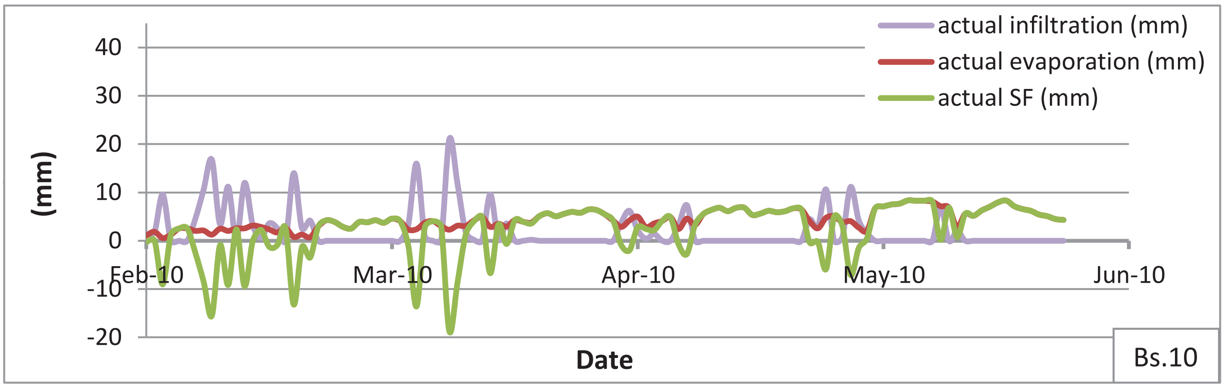

Figure 4-20. Comparison of actual infiltration, actual evaporation and actual SF for bare soil in 2010

In figure 4-20. The purple line represents the infiltration, the red line is the evaporation and the green line is the actual SF. In Figure 4-21 the green line in shows the actual SF, the cyan line is the BF and the dot blue line is the prescribed BPH. From the figure 4-21 we can see that the BF has the same pattern with the SF, it means that the surface condition was influencing the bottom condition. It may be because of the water table which was closer to the surface and the precipitation that makes the process more dynamic compared to 2009.

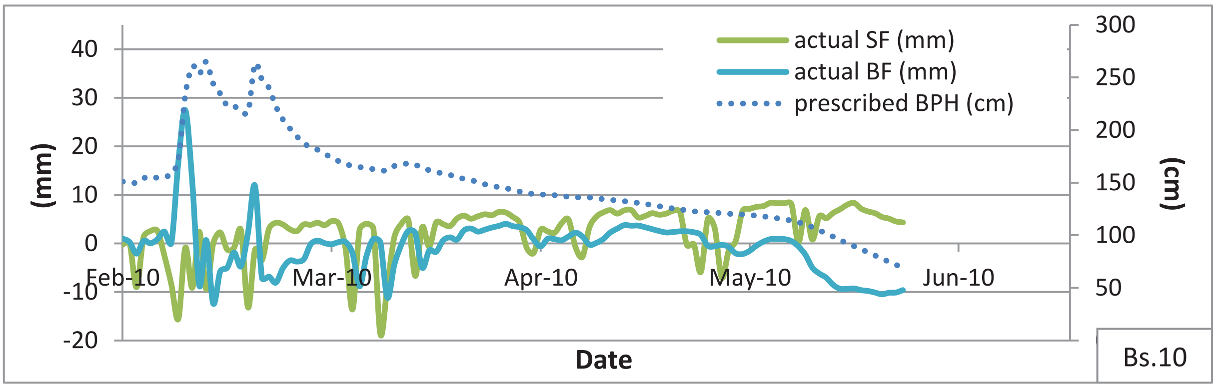

Figure 4-21. Comparison actual SF, actual BF and prescribed BHP for bare soil in 2010.

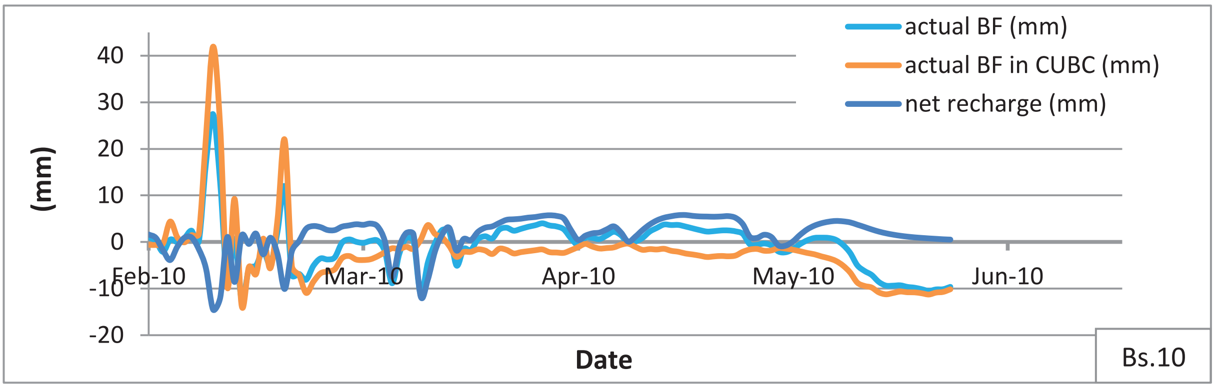

Figure 4-22. Comparison of actual BF, actual BF in CUBC and net recharge for bare soil in 2010.

To see only the effect of surface condition and not the effect of bottom pressure head to the BF, we compared the CUBC simulation with the normal simulation. In figure 4-22 the cyan line is the BF in normal simulation and the orange line is the BF in CUBC simulation. The difference between the two of them is the effect of climatic condition in the surface. The net recharge shows as the blue line in the figure 4-23.

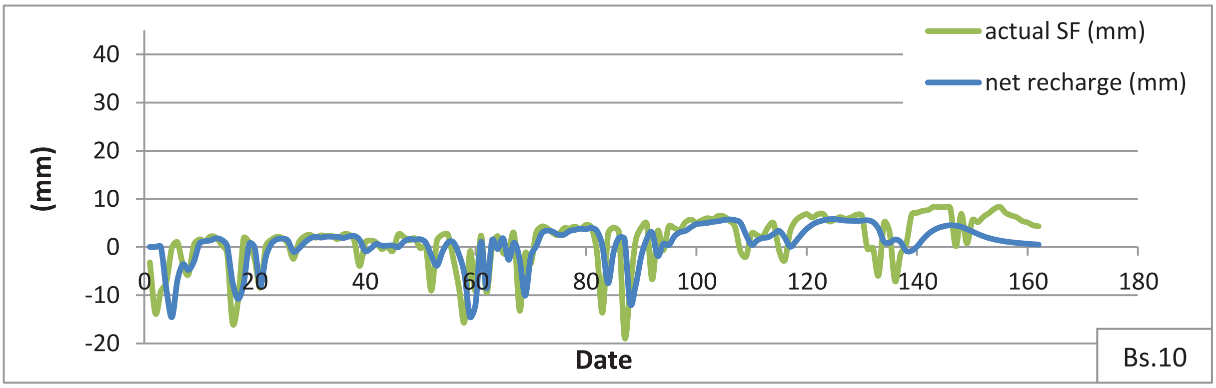

Figure 4-23. Comparison the actual surface flux and net recharge for bare soil in 2010.

### 4.3.6. *Quercus Ilex*-2010

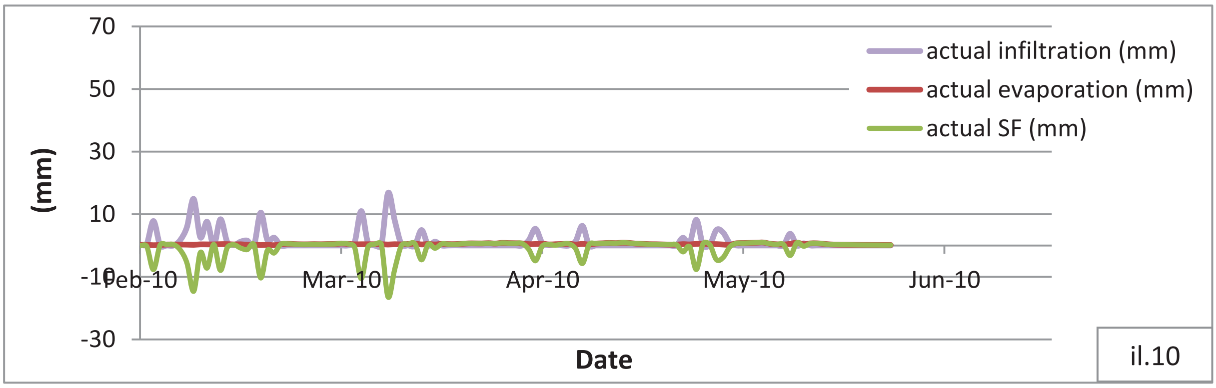

Figure 4-24. Comparison of actual infiltration, actual evaporation and actual SF for *Quercus ilex* in 2010

In figure 4-24 the purple line is representing the infiltration, the red line is the evaporation and the green line is the actual SF. The evaporation is also low compare to bare soil, similar reason as in 2009, because of the shading effect of the canopy that prevents the solar energy to be used to evaporate the available water.

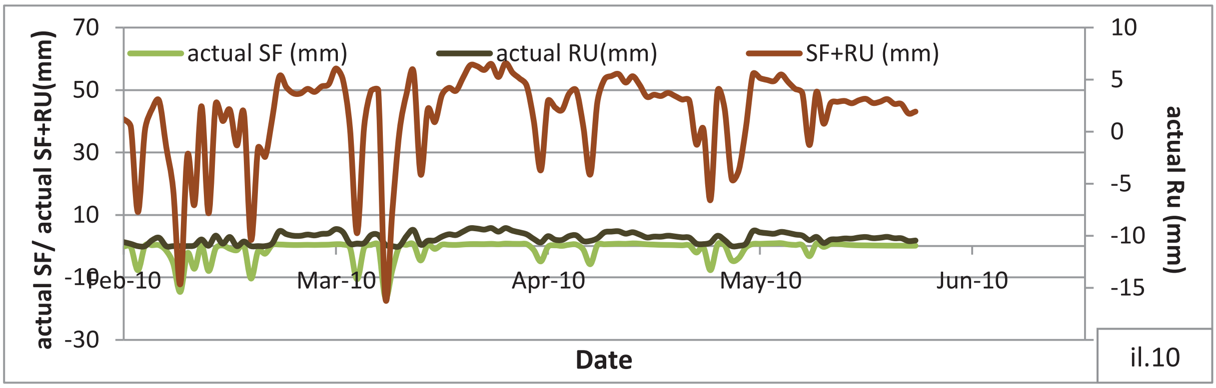

Figure 4-25. . Comparison the actual SF, actual RU and the SF+RU for *Quercus ilex* in 2010.

In the figure 4-25 the green line is the surface flux, the black line is the root water uptake (RU) and the brown line is the SF+RU. RU in *Quercuse ilex* is much higher than *Quercus pyrenaica* because it takes the water throughout the whole simulation period and has deeper root.

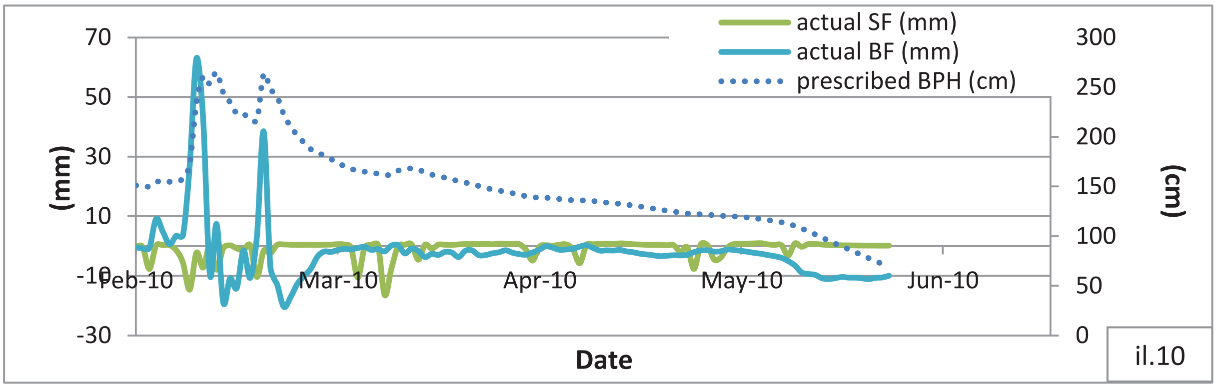

Figure 4-26. Comparison actual SF, actual BF and prescribed BHP for *Quercus ilex* in 2010.

In figure 4-26 we can see the comparison between actual SF, actual BF and prescribed PHB. Similar to bare soil, the actual BF is influenced by surface conditions and the prescribed BPH. The effect of surface condition can be seen in figure 4-27, the cyan line is the BF in normal simulation and the orange line is the BF in CUBC simulation. The net recharge is the blue line in figure 4-27. In Figure 4-28, we can see the comparison between actual SF to the net recharge. In February and March the net recharge has more positive value than in April till June due to higher precipitation in that period.

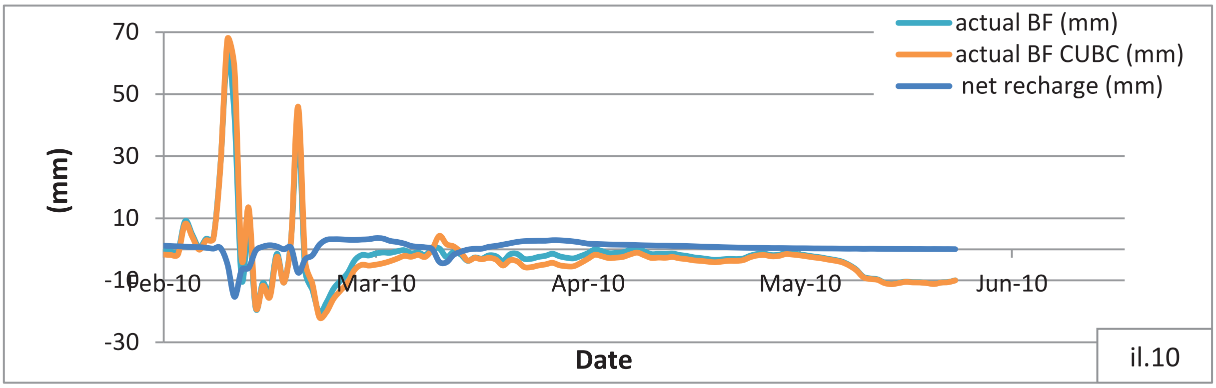

Figure 4-27. Comparison of actual BF, actual BF in CUBC and net recharge for *Quercus ilex* in 2010.

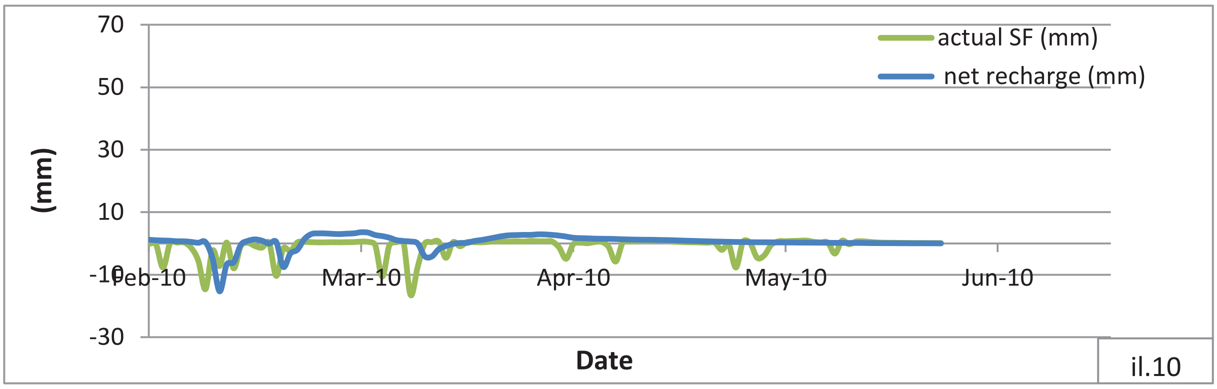

Figure 4-28. Comparison the actual surface flux and net recharge for *Quercus ilex* in 2010.

### 4.3.7. *Quercus pyrenaica-2010*

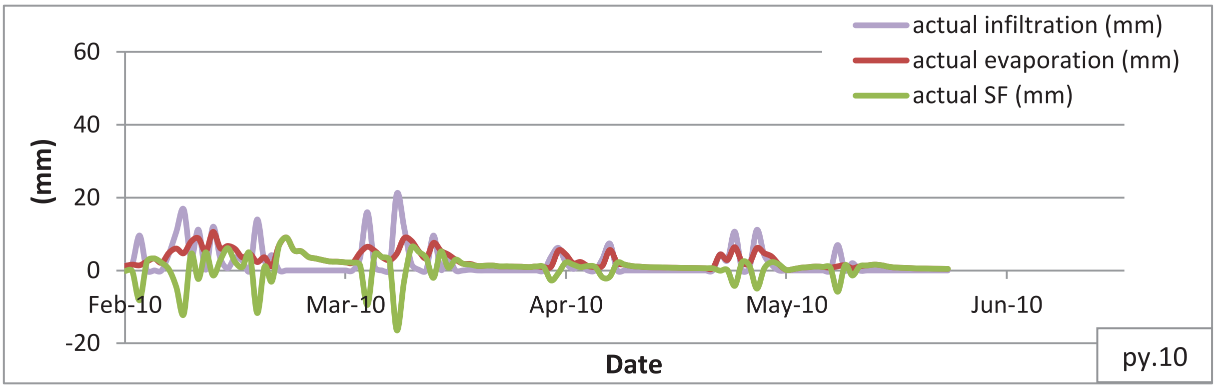

Figure 4-29. Comparison of actual infiltration, actual evaporation and actual SF for *Quercus pyrenaica* in 2010.

The purple line is representing the infiltration, the red line is the evaporation and the green line is the actual SF. Because the initial conditions for the soil are wetter than in 2009, the soil evaporates more than in 2009, where we can see low evaporation even though there is no shading effect until 15th of May.

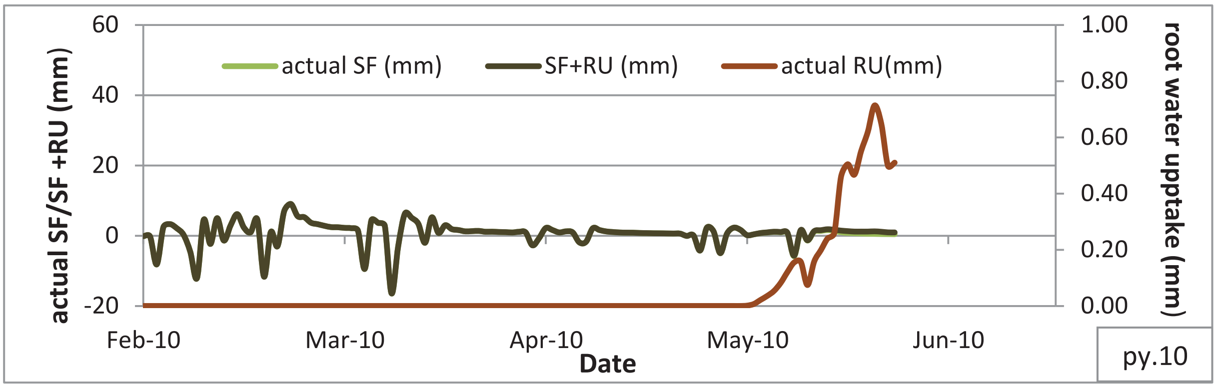

Figure 4-30. Comparison the actual SF, actual RU and the SF+RU for *Quercus pyrenaica* in 2010.

In the figure 4-30 the green line is the actual SF, the black line is the root water uptake (RU) and the brown line is the SF+RU. As mentioned before that in this simulation, for *Quercus pyrenaica* we assigned that it starts to take water in 15th of May, when it starts to develop leaves. Compared to 2009, the RU is higher because in 2010 there was more water available in the root zone.

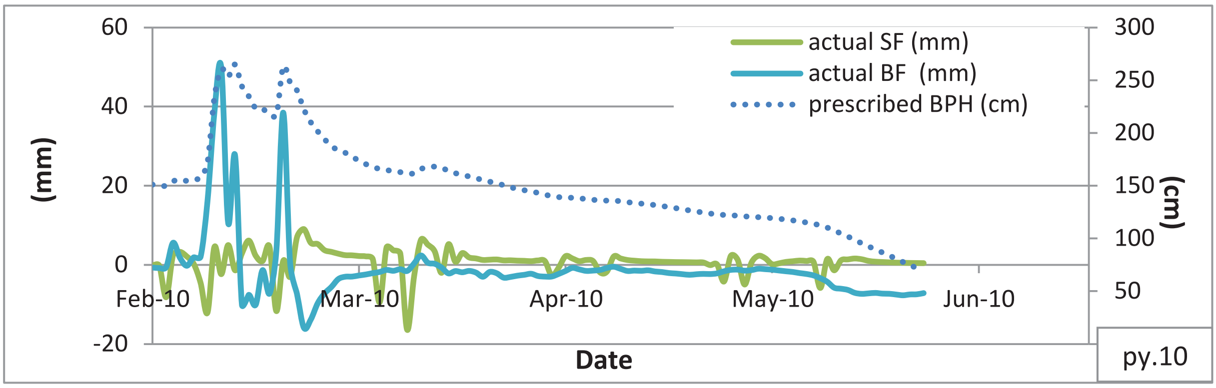

Figure 4-31. Comparison actual SF, actual BF and prescribed BHP for *Quercus pyrenaica* in 2010.

In figure 4-31 the green line in shows the actual SF, the cyan line is the BF and the dot blue line is the prescribed BPH. From the figure 4-32 we can see that he actual BF was influenced by the surface condition and also by the prescribed BPH.

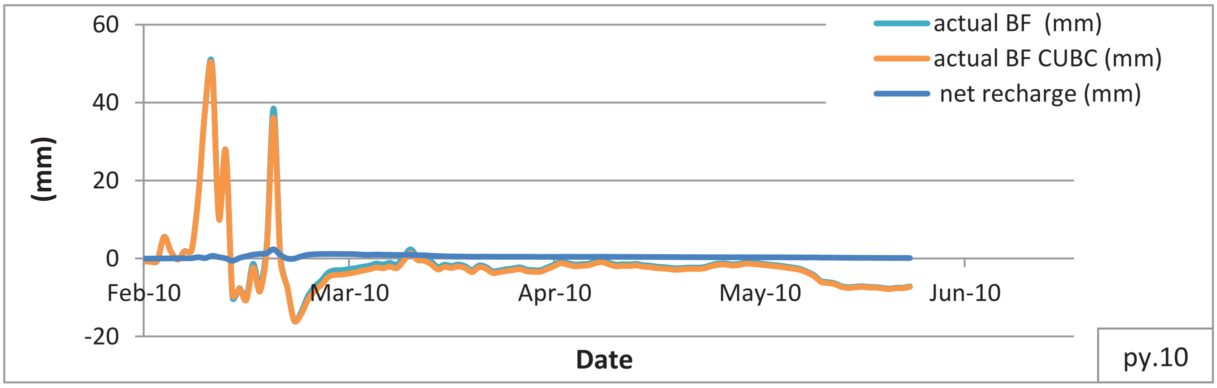

Figure 4-32. Comparison of actual BF, actual BF in CUBC and net recharge for *Quercus pyrenaica* in 2010.

In figure 4-32 the cyan line is the BF in normal simulation and the orange line is the BF in CUBC simulation. In2009 for *Quercus pyrenaica* the actual BF is influence more by the prescribed BPH, the two peak between February and March is due to the shallow of water table..

As we can see in figure 4-33 that water which passes the second node, from the precipitation, mostly didn't reached the bottom of the soil profile

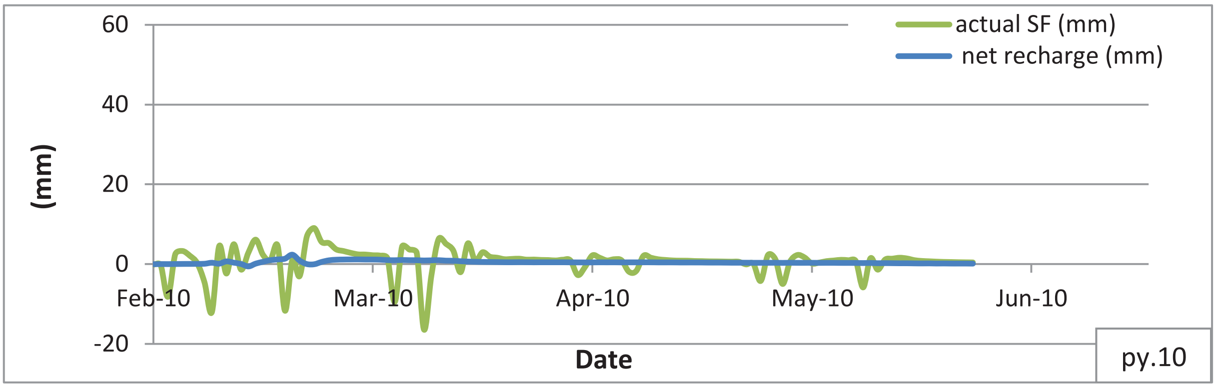

Figure 4-33. Comparison the actual SF and net recharge for *Quercus pyrenaica* in 2010.

### 4.3.8. Comparison water flow in 2009 and 2010

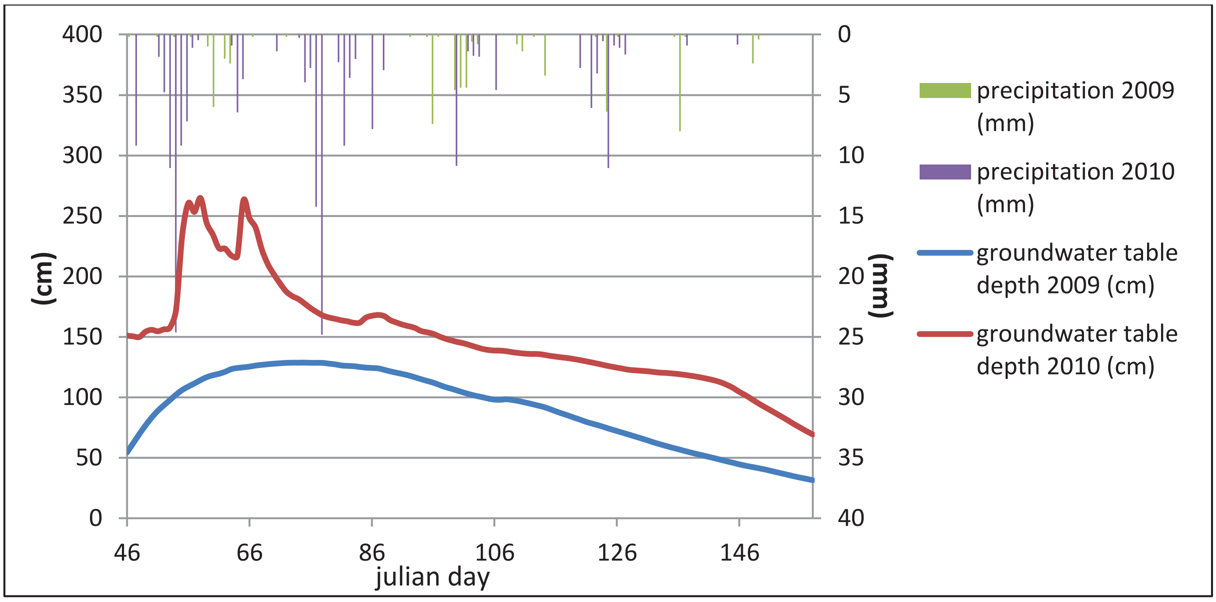

Figure 4-34. Precipitation and groundwater table depth in 2009 and 2010

In 2009, due to the interception by the canopy in *Quercus ilex*, the infiltration in *Quercus ilex* was lower than in the bare soil. Since *Quercus pyrenaica* had nearly no interception in the simulation persiods, therefore the infilration in *Quercus pyrenaica* was as much as in the bare soil. In 2009 evaporation in the bare soil was higher than both in *Quercus ilex* and *Quercus pyrenaica* but in *Quercus ilex* was lower than in *Quercus pyrenaica* because the dense canopy of *Quercus ilex* prevents the solar radiation to evaporate water. It is interesting that in generally leafless *Quercus pyrenaica*, despite cumulative infiltration in 2009 similar as compared to bare soil, had much lower cumulative evaporation than in bare soil (Table 4-5). This was because of different initial conditions, i.e. much drier soil under *Quercus pyrenaica* than of the bare soil.

The root water uptake in *Quercus ilex* is much higher than in *Quercus pyrenaica* since it takes the water along the simulation while for *Quercus pyrenaica* it starts to take water from 15th of May. Moreover the deeper and broader roots of *Quercus ilex* due to by larger canopy areas, also contributed to significantly larger water uptake.

In 2010 (Table 4-6), likewise in 2009, the cumulative infiltration in bare soil and *Quercus pyrenaica* was the same i.e., 240,33 mm, while in *Quercus ilex* was only 153,99 mm. due to the much larger interception by *Quercus ilex* reducing 86,40 mm of water. The cumulative evapotranspiration of bare soil was larger than of *Quercus pyrenaica* (also because of different initial conditions) but not as significantly as in 2009. The cumulative evaporation in *Quercus ilex* was much lower as compared to the other two land cover types, because of the canopy shadding effect which reduced almost ten times the evaporation as compared to bare soil. The wet conditions and the shallower water table in 2010 (Figure 4-34)made the root water uptake in both trees significantly larger in 2010 than in 2009.

Table 4-5. Water flow in the three land cover models in 2009.

| Bare soil 2009 | mm | | *Quercus ilex* 2009 | mm | | *Quercus pyrenaica* 2009 | mm | |
|---|---|---|---|---|---|---|---|---|
| cumulative infiltration | 59,27 | | cumulative infiltration | 32,65 | | cumulative infiltration | 59,27 | |
| cumulative evaporation | 400,04 | | cumulative evaporation | 32,40 | | cumulative evaporation | 60,24 | |
| cumulative SF | 340,77 | | cumulative SF | 4,70 | | cumulative SF | 0,96 | |
| | | | cumulative RU | 89,53 | | cumulative RU | 0,14 | |
| net recharge Rn=R-Eg | R | $E_g$ | net recharge Rn=R-$ET_g$ | R | $ET_g$ | net recharge Rn=R-$ET_g$ | R | $ET_g$ |
| | 0,21 | 203,5 | | 0,51 | 0,54 | | 0,3 | 0,32 |
| | Rn= -203,29 | | | Rn= -0,03 | | | Rn= -0,02 | |

Table 4-6. Water flow in the three land cover models in 2010.

| Bare soil 2010 | mm | | *Quercus ilex* 2010 | mm | | *Quercus pyrenaica* 2010 | mm | |
|---|---|---|---|---|---|---|---|---|
| cumulative infiltration | 240,33 | | cumulative infiltration | 153,99 | | cumulative infiltration | 240,33 | |
| cumulative evaporation | 497,80 | | cumulative evaporation | 48,67 | | cumulative evaporation | 319,88 | |
| cumulative SF | 257,48 | | cumulative SF | 105,31 | | cumulative SF | 79,55 | |
| | | | cumulative RU | 291,94 | | cumulative RU | 6,53 | |
| net recharge Rn=R-$E_g$ | R | $E_g$ | net recharge Rn=R-$ET_g$ | R | $ET_g$ | net recharge Rn=R-$ET_g$ | R | $ET_g$ |
| | 100,45 | 265,88 | | 57,01 | 115,91 | | 8,61 | 61,61 |
| | Rn= -165 | | | -58,90 | | | Rn= -53,0 | |

## 4.4. Spatial Distribution

The selected within the Sardon catchment net recharge zone (NRZ) is showed in figure 4-35. The total area of NRZ is 100339 $m^2$. In that area there are 3 land cover types each occupying the following area: bare soil area - 93889 $m^2$; *Quercus ilex* area - 4110 $m^2$; and *Quercus pyrenaica* area - 2340 $m^2$. The cumulative net recharge in NRZ for 2009 was -19087 $m^3$ and for 2010 is -15858 $m^3$. The negative values of net recharge in this area, for both selected years meant, that the ETg exceeded the recharge. This is understandable considering NRZ location in the discharge area of the Sardon catchment also confirmed by MODFLOW simulation carried out by Uria Carnejo (2000).

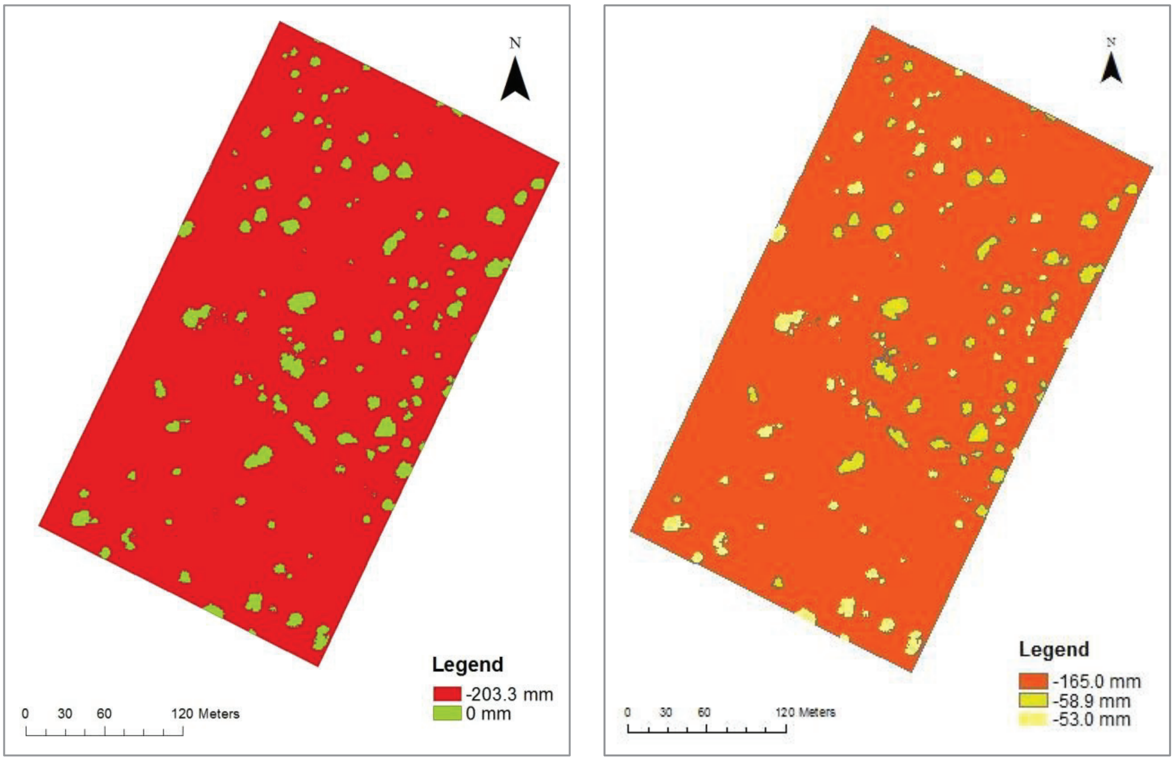

Figure 4-35. Spatial distribution of net recharge in 2009 (left) and 2010 (right).

Table 4-7. Water discharge in NRZ in 2009 and 2010 in 113 days start from 15th February until 7th June.

| | 2009 ($m^3$) | 2010 ($m^3$) |
|---|---|---|
| cumulative infiltration | 5838 | 23760 |
| cumulative evapotranspiration | 37833 | 47687 |
| cumulative SF | 32016 | 24794 |
| cumulative RU | 368 | 1215 |
| net recharge | -19087 | -15858 |

The table 4-7 shows the infiltration in 2010 is much higher than in 2009 due to higher precipitation. This high infiltration affects the amount of evaporation, because more water is available to evaporate. Moreover the water table in 2010 is closer to the surface than in 2009. These two factors cause the evaporation in 2010 is higher than in 2009. High evaporation in 2010 makes the value of net recharge negative eventhough the precipitation is high. The wet condition in 2010 is also affected the root water uptake. Because more water is available in 2010, the cumulative RU is also much higher in 2010 than in 2009.

.

# 5. CONCLUTIONS AND RECOMMENDATIONS

## 5.1. Conclutions

Net recharge depends on many factors such as water table depth, soil type, climatic conditions, land cover, etc. To assess the effect of land cover on the net recharge, we selected a ~1ha plot called net recharge zone (NRZ). The NRZ is an area where we assume that the soil is homogeneous (based on statistical analysis) and the water table depth is uniform. Therefore NRZ can be used to assess the dependency of net recharge on the land cover.

In each year of simulations, the value of net recharge varied depending on each land cover type. Land covers respond differently to precipitation. In the soil covered by *Quercus ilex* and *Quercus pyrenaica* (when it has leaves) the precipitation is intercepted by their canopies. Hence some of the water from precipitation is caught by surface storage (vegetation canopy) and evaporates before it reaches the soil. The effect of interception can be seen from the value of cumulative infiltration. For instance, in 2009 infiltration in bare soil (59,27 mm) is almost twice the infiltration of soil covered *by Quercus ilex* (32,65 mm).

A canopy of tree also influences the evaporation process. In the bare soil, solar radiation can directly reach the soil surface and evaporate the water in unsaturated zone or in saturated zone, whilst in soil covered by trees; a canopy prevents the solar radiation, reducing energy for evaporation. The tree parameter such as root depth, root distribution, LAI, affected the amount of root water uptake. The difference between these parameters makes the root water uptake of *Quercus ilex* and *Quercus pyrenaica* different. For example, in soil covered by *Quercus pyrenaica*, root water uptake was started in 15th of May in each year of simulation while for *Quercus ilex* it took up water through all the simulation.

This study proves that land cover has a significant impact on the net recharge to NRZ, so in the some land cover units within the Sardón catchment. However, the shallow water table in the NZR seems to have a great influence on the evaporation versus recharge balance. Therefore the result of this study may not be directly adapted to the entire Sardón catchment.

## 5.2. Recommendations

For further study related to this research the recommendations are:

- Groundwater table depth is important in quantifying net recharge, therefore to quantify net recharge in catchment scale it is important to divide the catchment based un uniformity of water table depth
- It is needed to study the impact of water table depth on the $ET_{g.}$
- Since tree and root parameters are important factors to differentiate root water uptake, it is important to determine these parameter carefully.
- Sensitivity analysis in needed to see the effect of each parameter on the results.
- The precipitation pattern needs to be studied in the study area thoroughly, in order to simulate the response of the model to the variability of the rain events. It is because the precipitation also influences the net recharge.
- It would be interesting and usefull to use developed Hydrus models to access the effect of climate change on net recharge in the study area as there are already indications of significant impact of climate change on groundwater resources in the Sardón study area.

# LIST OF REFERENCES

Agbakpe, B. A. (2010). *Estimating tree groundwater transpiration in La Mata catchment, Spain.* University of Twente Faculty of Geo-Information and Earth Observation (ITC), Enschede. Retrieved from http://www.itc.nl/library/papers_2010/msc/wrem/agbakpe.pdf

Anuraga, T. S., et al. (2006). Estimating groundwater recharge using land use and soil data: A case study in South India. *Agricultural Water Management, 84*(1-2), 65-76. doi: 10.1016/j.agwat.2006.01.017

Cisneros Vaca, C. R. (2011). *Simulation of groundwater recharge in the Sardon catchment, Spain.* University of Twente Faculty of Geo-Information and Earth Observation (ITC), Enschede.

Deme, G. (2011). *Partitioning subsurface water fluxes using coupled hydrus - modflow model : case study of La Mata catchment, Spain.* University of Twente Faculty of Geo-Information and Earth Observation (ITC), Enschede. Retrieved from http://www.itc.nl/library/papers_2011/msc/wrem/deme.pdf

Dripps, W. R., & Bradbury, K. R. (2007). A simple daily soil-water balance model for estimating the spatial and temporal distribution of groundwater recharge in temperate humid areas. *Hydrogeology Journal, 15*(3), 433-444. doi: 10.1007/s10040-007-0160-6

Effendi, I. (2012). *Evapotranspiration in dry climate area : comparing remote sensing techniques with unsaturated zone water flow simulation.* University of Twente Faculty of Geo-Information and Earth Observation (ITC), Enschede. Retrieved from http://www.itc.nl/library/papers_2012/msc/wrem/effendi.pdf

Feddes, R. A., & Raats, P. A. C. (2004). *Parameterizing the soil-water-plant root system* (Vol. 6).

Finch, J. W. (1998). Estimating direct groundwater recharge using a simple water balance model - sensitivity to land surface parameters. *Journal of Hydrology, 211*(1-4), 112-125. doi: 10.1016/s0022-1694(98)00225-x

Le Maitre, D. C., et al. (1999). A review of information on interactions between vegetation and groundwater. [Review]. *Water Sa, 25*(2), 137-152.

Llorono, M. S. (2000). Groundwater resources evaluation of Sardon catchment : Salamanca, Spain (pp. 65). Enschede: ITC.

Lubczynski, M. W. (2006). Fluxes, numerical models and sustainability of groundwater resources. *In: Sustainability of groundwater resources and its indicators : proceedings of a symposium held at Foz do Iguaçu, Brazil, April 2005 / ed. by Webb, B. ... et al. Wallingford : IAHS, 2006 (IAHS publications ; 302) ISBN 1-90150243-0. pp. 67-77.*

Lubczynski, M. W., & Gurwin, J. (2005). Integration of various data sources for transient groundwater modeling with spatio - temporally variable fluxes : Sardon study case, Spain. *JournalJournal of hydrology, 306*(1-4), 71-96.

Mualem, Y. (1976). A new model for predicting the hydraulic conductivity of unsaturated porous media. *Water Resources Research, 12*(3), 513-522. doi: 10.1029/WR012i003p00513

Mutasa, C. (2011). *Impacts of climate change on groundwater resources : a case study of the Sardon catchment, Spain.* University of Twente Faculty of Geo-Information and Earth Observation ITC, Enschede.

Ratnayake, R. M. S. (2000). Groundwater resources evaluation and grounwater modelling in hard rock terrain : Sardon catchment, Salamanca province, Spain (pp. 59). Enschede: ITC.

Reyes-Acosta, J. L., & Lubczynski, M. W. (2013). Mapping dry-season tree transpiration of an oak woodland at the catchment scale, using object-attributes derived from satellite imagery and sap flow measurements. *Accepted to Agricultural and Forest Management.*

Riano, D., et al. (2004). Estimation of leaf area index and covered ground from airborne laser scanner (Lidar) in two contrasting forests. *Agricultural and Forest Meteorology, 124*(3-4), 269-275. doi: 10.1016/j.agrformet.2004.02.005

Sala, A., et al. (1994). CANOPY STRUCTURE WITHIN A QUERCUS-ILEX FORESTED WATERSHED - VARIATIONS DUE TO LOCATION, PHENOLOGICAL DEVELOPMENT, AND WATER AVAILABILITY. *Trees-Structure and Function, 8*(5), 254-261.

Scanlon, B. R., et al. (2002). Choosing appropriate techniques for quantifying groundwater recharge. *Hydrogeology Journal, 10*(1), 18-39. doi: 10.1007/s10040-001-0176-2

Shakya, D. R. (2001). *Spatial and temporal groundwater modeling integrated with remote sensing and GIS : hard rock experimental catchment, Sardon, Spain.* ITC, Enschede.

Šimůnek, J., et al. (2012). *The HYDRUS-1D Software Package for Simulating the One-Dimensional Movement of Water, Heat, and Multiple Solutes in Variably-Saturated Media.* DEPARTMENT OF ENVIRONMENTAL SCIENCES UNIVERSITY OF CALIFORNIA RIVERSIDE.

Simunek, J., et al. (2012). HYDRUS: MODEL USE, CALIBRATION, AND VALIDATION. [Article]. *Transactions of the Asabe, 55*(4), 1261-1274.

Uria cornejo, S. P. (2000). *Groundwater recharge modelling in hard rocks area : Sardon case study, Spain.* ITC, Enschede.

van Genuchten, M. T. (1980). A Closed-form Equation for Predicting the Hydraulic Conductivity of Unsaturated Soils1. *Soil Science Society of America Journal, 44*(5), 892-898. doi: 10.2136/sssaj1980.03615995004400050002x

Vervoort, R. W., & Cattle, S. R. (2003). Linking hydraulic conductivity and tortuosity parameters to pore space geometry and pore-size distribution. [Article]. *Journal of Hydrology, 272*(1-4), 36-49. doi: 10.1016/s0022-1694(02)00253-6

Wang, Z., et al. (2000). Water-entry value as an alternative indicator of soil water-repellency and wettability. [Article; Proceedings Paper]. *Journal of Hydrology, 231*, 76-83. doi: 10.1016/s0022-1694(00)00185-2